

NIST Technical Note 2220

**The NIST 20 MW Calorimetry
Measurement System – Exhaust Flow
Calibration Using Tracer Gas Dilution**

Rodney A. Bryant

This publication is available free of charge from:
<https://doi.org/10.6028/NIST.TN.2220>

NIST
National Institute of
Standards and Technology
U.S. Department of Commerce

NIST Technical Note 2220

The NIST 20 MW Calorimetry Measurement System – Exhaust Flow Calibration Using Tracer Gas Dilution

Rodney A. Bryant
*Fire Research Division
Engineering Laboratory*

This publication is available free of charge from:
<https://doi.org/10.6028/NIST.TN.2220>

May 2022



U.S. Department of Commerce
Gina M. Raimondo, Secretary

National Institute of Standards and Technology
Laurie E. Locascio, NIST Director and Under Secretary of Commerce for Standards and Technology

Certain commercial entities, equipment, or materials may be identified in this document in order to describe an experimental procedure or concept adequately. Such identification is not intended to imply recommendation or endorsement by the National Institute of Standards and Technology, nor is it intended to imply that the entities, materials, or equipment are necessarily the best available for the purpose.

National Institute of Standards and Technology Technical Note 2220
Natl. Inst. Stand. Technol. Tech. Note 2220, 47 pages (May 2022)
CODEN: NTNOEF

This publication is available free of charge from:
<https://doi.org/10.6028/NIST.TN.2220>

Abstract

Exhaust flow measurements have been found to be a significant source of uncertainty for measurements of heat release rate in large-scale fire experiments. Asymmetric or skewed velocity distributions are often present in the exhaust ducts for open calorimetry systems used in large-fire research facilities, therefore making it difficult to measure exhaust flow accurately. Tracer gas dilution is a standard test method for determining volume flow in ducts. It is not sensitive to flow distribution and is derived from measurements independent of most flow monitoring techniques. Therefore, it is well suited for in-line calibrations of flow measurement devices in the exhaust ducts of facilities conducting large-scale fire experiments. For the first time, the method has been applied to calibrate the routine exhaust flow measurements at the National Fire Research Laboratory as a means to reduce the measurement uncertainty associated with open calorimetry systems. Measurement uncertainty for the calibration is estimated at 3 % and accounts for potential error due to incomplete mixing of the tracer. Multi-port sampling of the tracer, which is not part of the existing standard test method, is also demonstrated as a means to reduce the potential for measurement error due to incomplete mixing. Exhaust velocity and mass flow are necessary to compute heat release rate, and both are determined by averaging pitot probes installed in the exhaust ducts. An in-line calibration of the averaging pitot probes was conducted using tracer gas dilution. Measurement uncertainty for calibrated exhaust velocity and calibrated mass flow is estimated at 3 %. The in-line calibration of the exhaust flow measurement is an improvement over the accepted practice of comparing oxygen consumption calorimetry with heat release rate measured at a gas burner to develop a correction for the flow measurement. It is valid for a wide range of flow conditions and decouples measurement error between oxygen consumption calorimetry and fuel consumption calorimetry; therefore improving overall measurement accuracy for heat release rate.

Keywords

Tracer Gas Dilution; Flow Calibration; Heat Release; Oxygen Consumption Calorimetry; Constant-Injection; Photoacoustic Gas Detection; Flow Mixing; Duct Flows

Table of Contents

1. Introduction.....	1
2. Methods of Flow Measurement	2
2.1. Tracer Gas Dilution.....	2
2.2. Averaging Pitot Probes.....	3
3. Experimental Materials and Procedures.....	4
3.1. Flue Gas Exhaust System	4
3.2. Exhaust Flow Measurement – Averaging Pitot	7
3.3. Exhaust Flow Measurement - Tracer Gas Dilution.....	9
3.3.1. Optimizing Tracer Injection.....	13
3.4. Measurement Procedures.....	14
4. Results and Discussion	15
4.1. Measurement Uncertainty – Tracer Gas Dilution	15
4.1.1. Test for Sufficient Mixing	16
4.1.2. Estimated Uncertainty	21
4.2. In-Line Calibration of Averaging Pitot Probes.....	25
4.2.1. Calibrated Exhaust Flow Measurements	29
5. Summary	31
References.....	33
Appendix A: Nomenclature	36
Appendix B: Detailed Uncertainty Budgets	37

List of Tables

Table 1 Details of the canopy hoods and exhaust system.....	5
Table 2 Probe coefficients for the averaging pitot probes.	8
Table 3 Effective diameter of NFRL's exhaust ducts	9
Table 4 Results of experiments to test for sufficient mixing. The relative standard deviation of the average volume flow ratio across experiments with different injection locations provides an estimate of the potential for measurement error due to inadequate mixing.....	20
Table 5 Estimated uncertainty for measurements of volume flow in the NFRL exhaust system using tracer gas dilution.	24
Table 6 Flow calibration constants determined from the in-line calibration of the averaging pitot probes using tracer gas dilution.	28
Table 7 Estimated uncertainty for flow measurements in the NFRL exhaust system using the averaging pitot probes.	31

Table B.1 Example of an uncertainty budget for the volume flow determined using TGD at the 3 MW calorimeter.....38

Table B.2 Example of an uncertainty budget for effective exhaust velocity measured at the averaging pitot probes.39

Table B.3 Example of an uncertainty budget for exhaust mass flow measured at the averaging pitot probes.40

List of Figures

Figure 1 Conceptual schematic of the method for tracer gas dilution.....3

Figure 2 Generic configuration and installation for an averaging pitot probe.....4

Figure 3 NFRL’s flue gas exhaust system.6

Figure 4 Installation of two averaging pitot probes in NFRL's 2.424 m exhaust duct. Photograph view is upstream.7

Figure 5 Experimental setup of the tracer gas dilution method, constant-injection technique. Dark brown arrows indicate pure SF₆, light brown arrows indicate diluted/trace amounts of SF₆.10

Figure 6 Tracer injection ring (left photo); and injection ring mounted at the inlet of the exhaust duct (right photo).11

Figure 7 Installation of two averaging pitot probes and the gas sampling tube in the 1.975 m exhaust duct. Photograph view is upstream and into the flow.....12

Figure 8 Estimates of tracer injection volume flow required to generate optimal tracer volume fractions downstream. Reference conditions for volume flow are 273.15 K and 101325 Pa.14

Figure 9 Time trace of a typical experiment. Simultaneous measurements of volume flow using the averaging pitot probes (APP) and the TGD method are shown on the left vertical axis. Volume flow of the injected tracer is shown on the right vertical axis.....15

Figure 10 Schematic to demonstrate the impact of injection position of the tracer on the distribution of tracer for downstream locations at un-mixed and mixed conditions, using either a multi-port sample (MPS) or single point traverse (SPT).17

Figure 11 Time trace for a steady exhaust setpoint and tracer injection flow demonstrate TGD providing a steady measurement of exhaust flow during relocation of the tracer injection point at the inlet plane. Brackets indicate location of tracer injection point.18

Figure 12 Confirmation of sufficient mixing of the tracer with single point injection for various locations at the exhaust duct inlet. Each point is the mean of 10 or more measurements and the error bars represent the standard deviation of the mean (SDOM). The solid and dashed horizontal lines represent the overall mean and standard deviation, respectively, of the volume flow computed from the 6 locations.19

Figure 13 Locations (arrows) of the tracer injection ring for the 10 MW and 20 MW calorimeters.....20

Figure 14 Measurement uncertainty estimates of volume flow determined using TGD at the exhaust ducts of the 0.5 MW and 3 MW calorimeters. The dashed line represents the average uncertainty for the range of volume flow during routine operations.22

Figure 15 Measurement uncertainty estimates of volume flow determined using TGD at the exhaust ducts of the 10 MW and 20 MW calorimeters. The dashed line represents the

average uncertainty for the range of volume flow during routine operations (Lower limit is 1200 m³/min for the 20 MW calorimeter).23

Figure 16 Results of flow calibration experiments at the 0.5 MW and 3 MW calorimeters. The ratio of volume flow measured using tracer gas dilution and averaging pitot probes are shown. The solid line represents the average ratio over the operational range of flow for each calorimeter.26

Figure 17 Results of flow calibration experiments at the 10 MW and 20 MW calorimeters. The ratio of volume flow measured using tracer gas dilution and averaging pitot probes are shown. The solid line represents the average ratio over the operational range of flow for each calorimeter.27

Figure 18 Calibrated mass flow for the 3 MW calorimeter. Shaded region represents the estimated expanded uncertainty.30

1. Introduction

The heat released from burning items is a central measurement for large-scale fire testing and the primary measurement for estimating the magnitude of the fire hazard. Oxygen consumption calorimetry is the most widely used method for measuring the rate of heat release, \dot{Q}_{OC} , during a large fire experiment. Quantitative determination of the rate of heat release rate, Eq. (1), requires complete capture of the fire plume and the measurement of at least two quantities from the exhaust stream (flue gas): oxygen volume fraction, X_{O_2} , and total gas flow, \dot{V}_e . [1]

$$\dot{Q}_{OC} = (\Delta_c H_{fuel})_{O_2} \dot{V}_e (X_{O_2}^o - X_{O_2}) \quad (1)$$

Accurate measurements of both quantities are necessary to achieve an accurate measure of heat release rate. Multiple studies have cited the exhaust flow measurement as a significant source of uncertainty when measuring the rate of heat release. [2-7] Accurate measurement of the exhaust flow in large fire calorimeters is difficult due to potential lack of symmetry of the flow profiles in the large exhaust ducts. Consensus standards for open calorimetry fire testing, such as ASTM E2067, ISO 24473, and NFPA 286, provide guidance in the form of a heat release rate calibration (overall system calibration) that accounts for the error of the flow measurement. For example, in uses of an orifice plate as the flow measurement device, the systematic error of the heat release rate measurement and more explicitly the error of the exhaust flow measurement is inferred by comparing the rate of heat release from a gas burner – using fuel consumption calorimetry, to that measured in the exhaust flue by oxygen consumption calorimetry. The error is used to estimate the flow coefficient for the orifice plate and hence apply a correction to the flow measurement (ASTM E2067, ISO 24473); or it is used directly to correct the measurement of heat release rate by oxygen consumption calorimetry (ASTM E1354, ASTM E2257). [8-11]

Correcting the flow measurement based on the comparison with heat release rate determined by fuel consumption calorimetry, therefore a gas burner, is practical but not ideal. This practice couples any error in determining heat content and fuel flow at the burner with that of the calorimeter. Conducting an in-situ calibration of the device for measuring exhaust flow is best practice. ASTM E2067 and ISO 24473 recommend, but do not require, an in-situ calibration of the flow measurement device (bi-directional probe or the orifice plate) by conducting a velocity traverse across the exhaust duct to determine the flow distribution. The calibration constant, the ratio of the average velocity determined from the distribution measurement to the centerline (or orifice plate) measurement, becomes the correction for flow measurement.

Another technique for conducting in-situ calibrations of flow measurement devices used in exhaust ducts is tracer gas dilution (TGD). The method is used to infer the volume flow in the exhaust duct from measurements of the known amount of tracer injected into the flow at an upstream location and measurements of the diluted tracer concentration sampled from a downstream location. The method is not sensitive to irregular or skewed velocity distributions in the duct and is therefore well suited for in-situ calibrations. It is a standard test method described by ASTM E2029 and used to determine volume flow when conventional flow devices such as pitot probes do not provide accurate measure of volume flow.

This report will describe the methodology and equipment used to conduct an in-line calibration of a measurement device for exhaust flow in a large fire calorimeter, using tracer gas dilution. Averaging pitot probes (APP) have been installed in the exhaust ducts of the National Fire Research Laboratory (NFRL) to provide routine measurements of exhaust flow during large fire experiments. These devices are off-the-shelf technology widely used to monitor flows for industrial processes. Details of their application in the NFRL have been described in previous publications [12, 13] and will be summarized here.

2. Methods of Flow Measurement

Many methods exist to measure flow in ducts. Examples include pressure impact probes (e.g. pitot tubes, bi-directional probes, and averaging pitot tubes), hot-wire anemometers, ultrasonic flow meters, and orifice plates. The accuracy of these methods is limited when less-than-ideal flow characteristics exist, such as: asymmetric velocity distribution, off-axis flow components due to swirl, turbulence, very low flow, and flow reversal due to wakes or buoyancy. These conditions are often encountered when the methods are applied in ducts with short lengths of straight section upstream and downstream of the measurement location. Specifying volume or mass flow using these methods also require a measurement of cross-sectional area which can be a significant source of uncertainty if the shape and dimensions of the sampling section cannot be determined with sufficient accuracy.

Two measurement methods are considered, tracer gas dilution (TGD) and averaging pitot probes (APP). Tracer gas dilution is a volumetric or whole field method that infers volume flow. The method does not require measurement of the cross-sectional area of the duct, and it is not sensitive to the non-ideal flow characteristics mentioned previously (with the exception of flow reversal). Averaging pitot probes determine average flow velocity along a chord length of the exhaust duct (length of the probe) from a measurement of the difference between total and static pressure at the device. Combined with a measurement of the exhaust duct diameter (cross-sectional area), volume flow in the exhaust duct can be computed. Volume flow measurements inferred from tracer gas dilution and the averaging pitot probes are independent as they are derived from independent measurements – tracer volume flow and volume fraction vs differential pressure and duct diameter. Therefore, the tracer gas dilution method is ideal for the in-line calibration of the averaging pitot probes.

A summary of both measurement concepts is described below. In addition, a detailed description of the equipment and experiment procedures is described in later sections. Further background information on the two methods has been provided in previous publications. [13, 14]

2.1. Tracer Gas Dilution

The method for tracer gas dilution as described by ASTM Standard E2029 uses the constant-injection technique, assuming an ideal gas and constant flow. [15] For this technique, a known concentration of tracer is injected at a constant rate into an upstream location of the flow stream. The tracer becomes mixed and diluted in the flow stream. At a downstream location, samples of the gas mixture are extracted from the flow stream and transported to an analyzer to measure the diluted volume fraction of tracer gas.

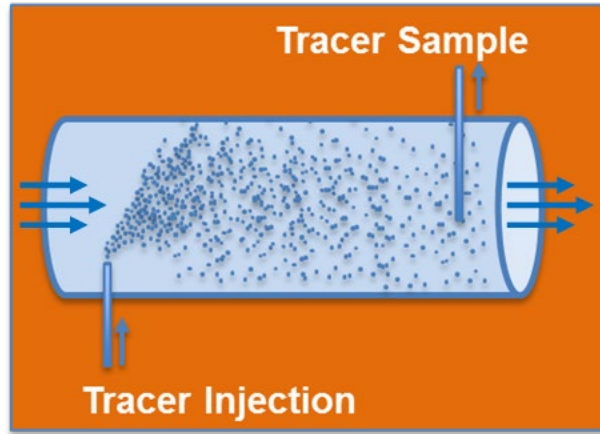


Figure 1 Conceptual schematic of the method for tracer gas dilution.

The constant-injection technique requires precise metering of the injected tracer, sufficient mixing of the tracer into the transport stream, and accurate detection of the diluted tracer. When these requirements are satisfied, the volume flow in the duct is given by the following equation:

$$\dot{V} = \frac{X_{T,I} - X_{T,D}}{X_{T,D} - X_{T,U}} \dot{V}_{T,I} \quad (2)$$

where $X_{T,I}$ is the known volume fraction of the injected tracer; $X_{T,D}$ is the volume fraction of the diluted tracer measured at the downstream sample location; $X_{T,U}$ is the volume fraction of the tracer measured upstream of the injection point or in the ambient environment; and $\dot{V}_{T,I}$ is the measured volume flow of the injected tracer. In the case of a pure tracer, $X_{T,I} = 1.00$.

2.2. Averaging Pitot Probes

Averaging pitot probes (also known as flow-averaging tubes or multi-port averaging pitot tubes) are impact pressure devices that measure the difference between total and static pressure, ΔP , induced by a flowing gas or liquid. Like the standard pitot tube, Bernoulli's principle is used to infer the fluid velocity from measurements of pressure differential and fluid density, ρ . The averaging pitot extends across the entire diameter of the pipe and has multiple impact and static ports positioned at equal annular locations, Figure 2. The number of impact ports and their spacing can be designed to meet specific applications, but they are usually spaced to account for a log-linear distribution of velocity. [16] Averaging of the spatial distribution of pressure occurs inside the impact and static chambers built into the probe, resulting in a measurement of differential pressure that represents the mean gas velocity along the chord, V_c . This relationship is described in the following equation, where K_a is the flow coefficient for the averaging pitot, ranging from 0.6 to 0.8. [17]

$$V_c = K_a \sqrt{\frac{2 \Delta P}{\rho}} \quad (3)$$

This velocity measurement is combined with a measurement of the diameter, D , of the exhaust duct (cross-sectional area) to determine volume flow.

$$\dot{V}_e = V_c \frac{\pi D^2}{4} \quad (4)$$

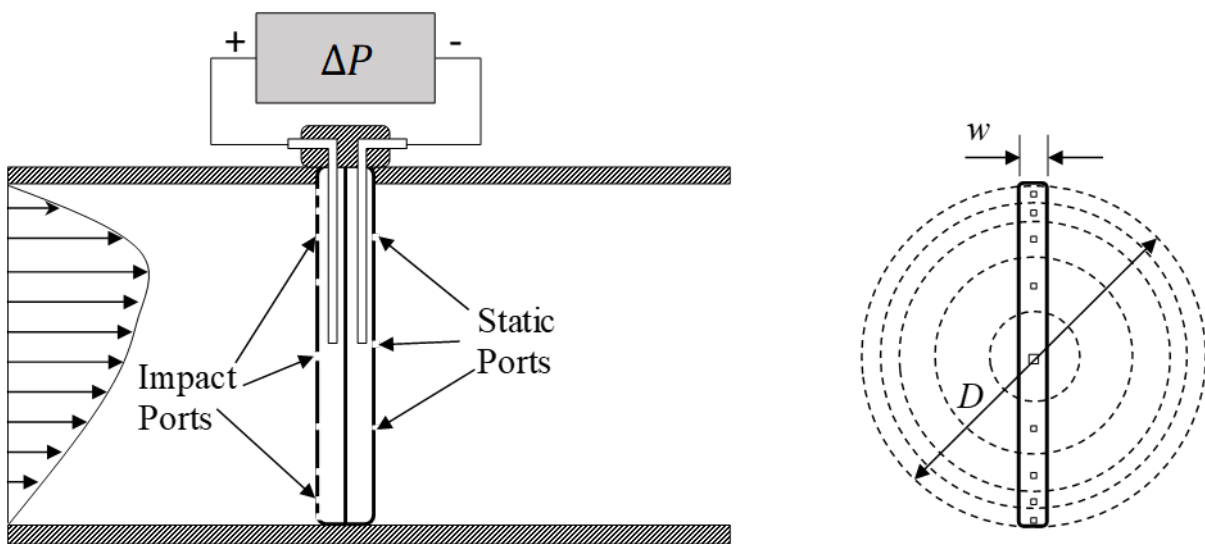


Figure 2 Generic configuration and installation for an averaging pitot probe.

3. Experimental Materials and Procedures

A detailed description of the materials and instrumentation that form NFRL's 20 MW Calorimetry System has been provided in Technical Note 2077. [12] Relevant descriptions are repeated here while others are summarized for brevity.

3.1. Flue Gas Exhaust System

Large-canopy exhaust hoods are utilized to capture the fire effluents for quantification of heat release rate as a function of time. The insulated steel hoods are suspended above the test floor and serviced by large exhaust ducts that transport the combustion products to an emissions control system (ECS) for conditioning before release into the atmosphere. The facility has 4 canopy hoods and hence 4 oxygen consumption calorimeters. Each calorimeter is denoted by its fire capacity, 0.5 MW, 3 MW, 10 MW, and 20 MW. Details of each canopy hood and its associated exhaust path are listed in Table 1.

Table 1 Details of the canopy hoods and exhaust system.

Canopy Hood m x m	Duct ID m	Flow Capacity kg/s (m³/min)*	Fire Capacity MW
3.1 × 3.2	0.483	4.3 (200)	0.5
6.1 × 6.1	1.975	27.5 (1275)	3
8.4 × 12.4	1.975	58.2 (2700)	10
13.8 × 15.4	2.424	116 (5400)	20

* Reference conditions for volume flow are 273.15 K and 101325 Pa.

The 3 MW and 10 MW calorimeters are serviced by the same exhaust duct with inner diameter (ID) 1.975 m, and the 20 MW calorimeter is serviced by a 2.424 m ID duct. A 0.483 m ID exhaust duct services the 0.5 MW calorimeter and feeds into the 1.975 m duct. Both large ducts, 1.975 m and 2.424 m, run along the roof of the facility and transport the combustion products from the fire to the ECS, as shown in Figure 3. Instrument measurement stations are located upstream of the ECS. At these locations, measurements of gas volume fraction, gas temperature, and gas velocity are made to determine heat release rate. The layout of the roof ducts was designed to provide more than 10 diameters of straight run to create a well-developed flow at the measurement stations. Flow is pulled through the exhaust system by induced draft fans near the end of the system. Therefore, the operating pressure in the ducts is slightly below atmospheric. The system has a mass flow capacity of approximately 116 kg/s (5400 m³/min at reference conditions of 273.15 K and 101325 Pa) and a heat release rate capacity of 20 MW.

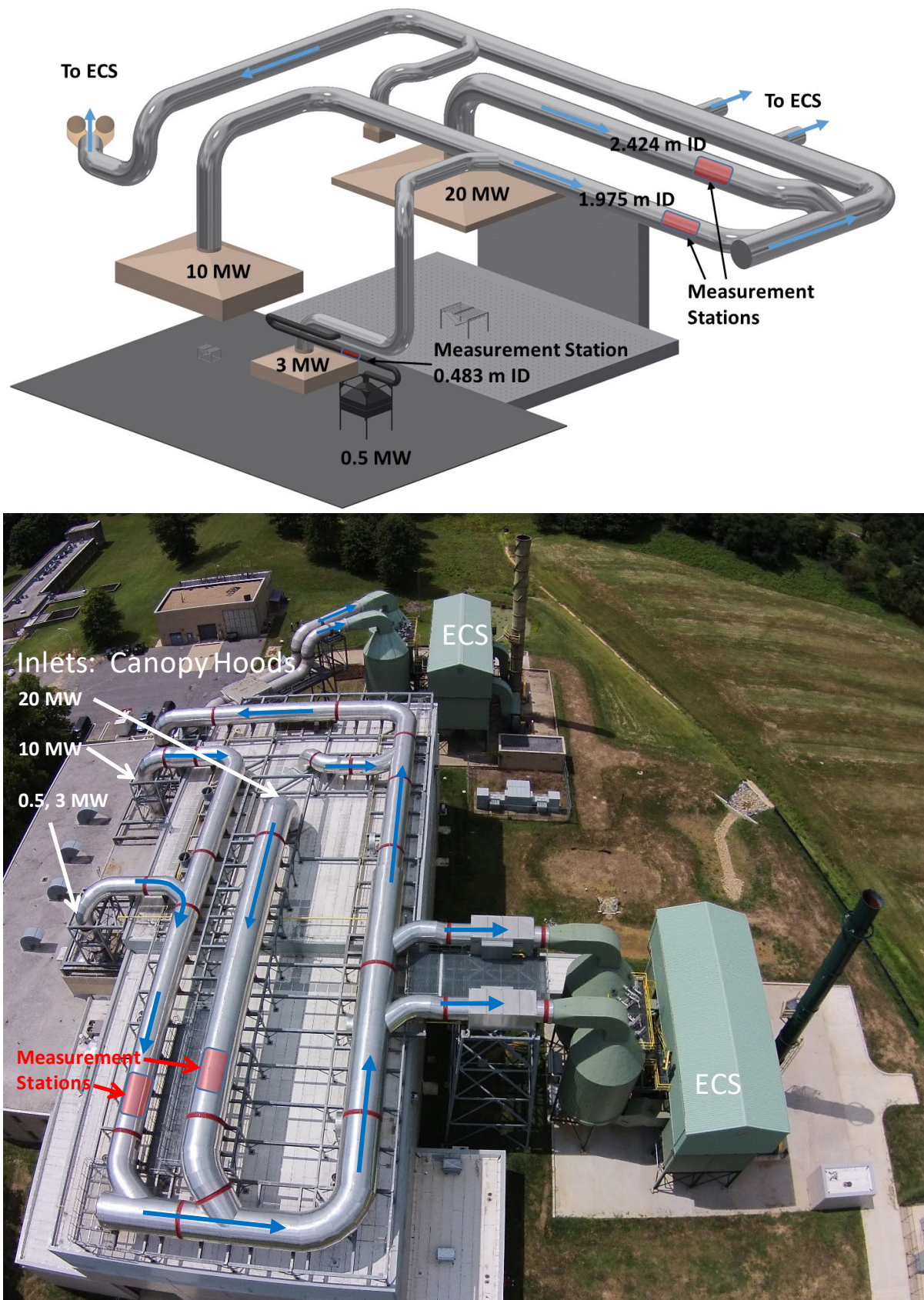


Figure 3 NFRL's flue gas exhaust system.

3.2. Exhaust Flow Measurement – Averaging Pitot

The flow sensors used in the exhaust ducts are tee-shaped averaging pitot style probes (Rosemont 485 Annubar)¹. The probes are made of 316 stainless steel and have a width of 2.692 cm. Three probe lengths (0.48 m, 1.97 m, and 2.42 m) are used to match the inner diameter of the exhaust ducts. Separate pairs of pitot probes, each equipped with two bare bead thermocouples (Type K), are installed in the 1.975 m duct and the 2.424 m duct. The two probes are installed on orthogonal chords (A and B) of the duct cross section and 45° relative to horizontal as shown in Figure 4. Minimum separation distance between the two probes is one duct diameter. The average velocity for two probes, chord A and chord B, is reported as the flow velocity measured in the exhaust duct:

$$V_{e,avg} = \frac{V_{e,A} + V_{e,B}}{2} \quad (5)$$

A single averaging pitot probe and thermocouple pair are installed vertically (chord A) in the 0.483 m duct for the 0.5 MW calorimeter, hence $V_{e,avg} = V_{e,A}$.

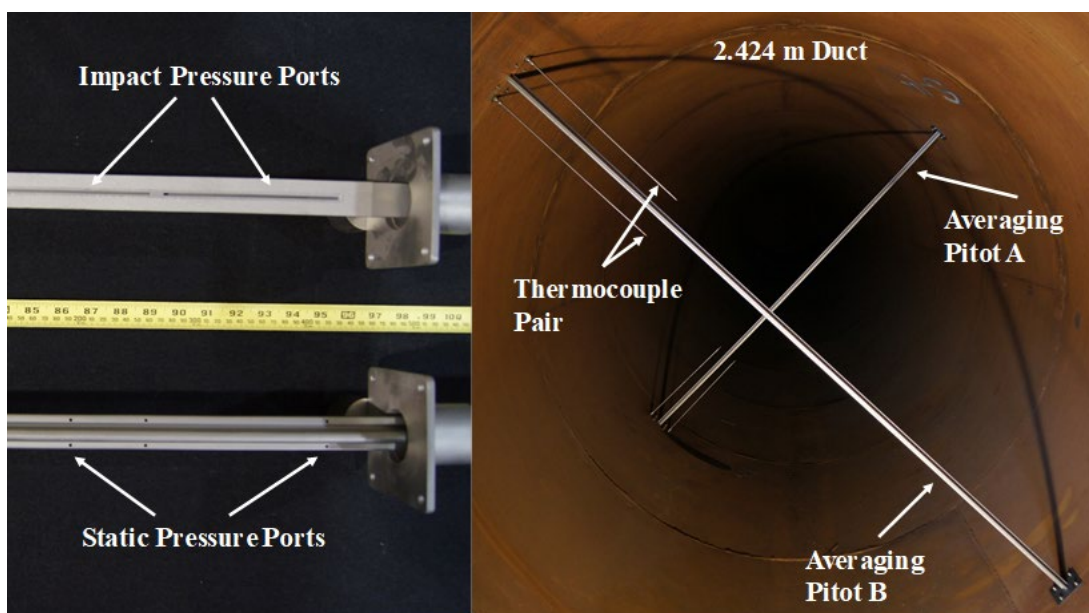


Figure 4 Installation of two averaging pitot probes in NFRL's 2.424 m exhaust duct. Photograph view is upstream.

The pressure differential, ΔP , induced by flow across the averaging pitot probes is measured with high-precision capacitance manometers (MKS 220D Baratron). The instruments have a range of 0 Pa to 1333.2 Pa and are calibrated against an in-house working standard for pressure

¹ Certain commercial entities, equipment, or materials may be identified in this document in order to describe an experimental procedure or concept adequately. Such identification is not intended to imply recommendation or endorsement by the National Institute of Standards and Technology, nor is it intended to imply that the entities, materials, or equipment are necessarily the best available for the purpose.

(NFRL WSTD 577967). The relative expanded uncertainty² of the differential pressure measurement is estimated at 0.6 %. Gas density at each averaging pitot probe, $\rho_{e,i}$, is derived from temperature measurements at the two bare-bead thermocouples mounted at the probe. Type K thermocouples are used to estimate gas temperature with an estimated relative expanded uncertainty 1.0 %. The ambient pressure, P_{amb} , inside the facility is measured with a digital barometer (Vaisala PTB220) with an expanded uncertainty of 103 Pa. The molecular weight, M_e , of the exhaust gas is assumed to be equal to that of the dry ambient air, (28.97 ± 0.10) kg/kmol. Only cold flow experiments using the ambient air were run, making this an appropriate assumption. The measured output of each capacitance manometer, thermocouple pair, and the digital barometer is used to compute the flow velocity, $V_{e,i}$, at each device i ($i = A$ or B).

$$V_{e,i} = K_{a,i} \sqrt{\frac{2\Delta P_i}{\rho_{e,i}}} \quad (6)$$

The flow coefficient, K_a , for the probe was provided by the manufacturer, with an estimated expanded uncertainty of 0.75 %, Table 2. This estimate is valid for the case of fully-developed turbulent pipe flow, with Reynolds number (Re) greater than 12 500 for flow over the probe. Larger errors in the flow measurement may occur if these conditions are not met. If so, the manufacturer recommends an in-line calibration of the probe to improve measurement accuracy. [18]

Table 2 Probe coefficients for the averaging pitot probes.

Probe Length, m	K_a	Calorimeter
0.48	0.6055 ± 0.0045	0.5 MW
1.97	0.6271 ± 0.0047	3 MW 10 MW
2.42	0.6283 ± 0.0047	20 MW

Mass flow is routinely monitored and reported for NFRL's calorimetry system. For the purpose of comparison with the tracer gas dilution method, volume flow, \dot{V} , is reported as follows:

$$\dot{V}_{e,APP} = V_{e,avg} \frac{\pi D_{eff}^2}{4} \quad (7)$$

² Unless otherwise stated, all uncertainty values are reported as expanded uncertainty, for a 95% confidence interval with a coverage factor $k = 2.0$.

The effective inner diameter for each exhaust duct, D_{eff} , is listed in Table 3. It was computed from a series of chord measurements made inside each duct. [12, 13]

Table 3 Effective diameter of NFRL's exhaust ducts

Calorimeter	D_{eff} , m
0.5 MW	0.483 ± 0.004
3 MW, 10 MW	1.975 ± 0.005
20 MW	2.424 ± 0.009

3.3. Exhaust Flow Measurement - Tracer Gas Dilution

A constant-injection system for tracer gas dilution measurements was assembled and integrated into NFRL's flue gas exhaust and gas sampling systems. Tracer was injected at the inlet of the exhaust duct (the canopy hood) and sampled at the flow measurement station using the facility's existing gas sampling and gas conditioning equipment. [12] A schematic of the constant-injection system is shown in Figure 5.

The tracer, sulfur hexafluoride (SF_6 , $99.99\% \pm 0.02\%$), was injected at the inlet of the exhaust duct. A coiled copper tube served as a heat exchanger to ensure the tracer was at ambient temperature when it entered the flow control and flow measurement devices. Volume flow of the injected tracer was adjusted using a mass flow controller (MKS Instruments, Inc.; Model: M100B53CS1BV, 0-5 L/min). The injection flow was precisely measured using a laminar flow element (Fluke; Model: molbloc-L 1E3-VCR-V-Q with molbox1 terminal) located downstream of the mass flow controller. The laminar flow element has a standard uncertainty of 0.07 % of flow reading for SF_6 , as demonstrated by comparisons against NIST PVTt primary flow standards (NIST 34 L Pressure Volume Temperature and Time Primary Flow Standard). [19] Reference conditions for volume flow from the laminar flow element system are 273.15 K and 101325 Pa. All volume flow measurements reported here are referenced to these conditions.

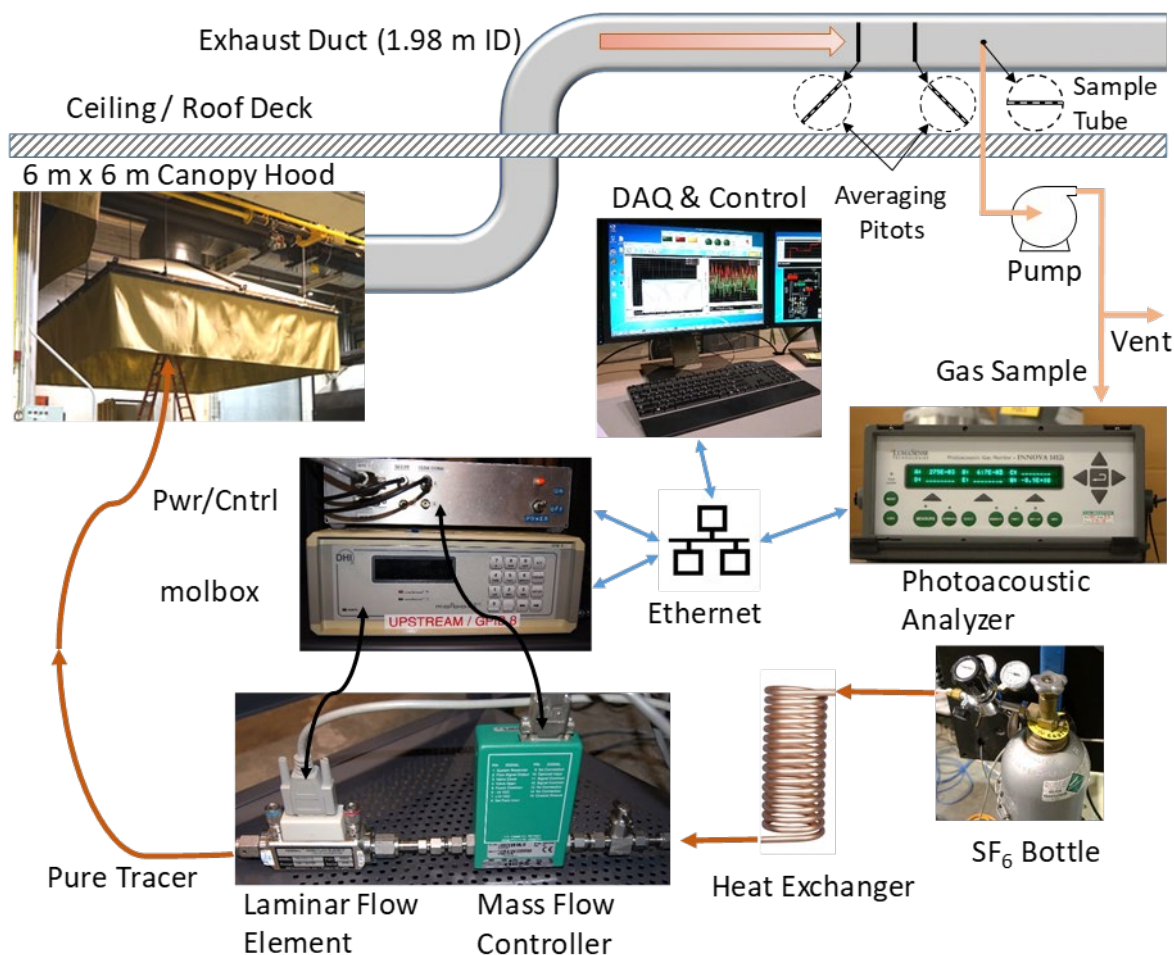


Figure 5 Experimental setup of the tracer gas dilution method, constant-injection technique. Dark brown arrows indicate pure SF₆, light brown arrows indicate diluted/trace amounts of SF₆.

Tracer was released into the exhaust duct using an injection ring made from 6.35 mm (0.25 in) copper and stainless-steel tubing, Figure 6. The ring was 35.6 cm (14 in) in diameter, with 3.18 mm (0.125 in) diameter holes spaced apart by 50.8 mm. The injection system was checked for leaks by charging the system with pure tracer up to the point of the mass flow controller; closing the ball-valve; and then confirming that the tracer was not detected in the exhaust flow. Leaks in the injection system, upstream of the metering device, will bias the flow measurement toward lower values. In general, unusually low flow measurements should be investigated as they could be the result of leaks in the injection system.

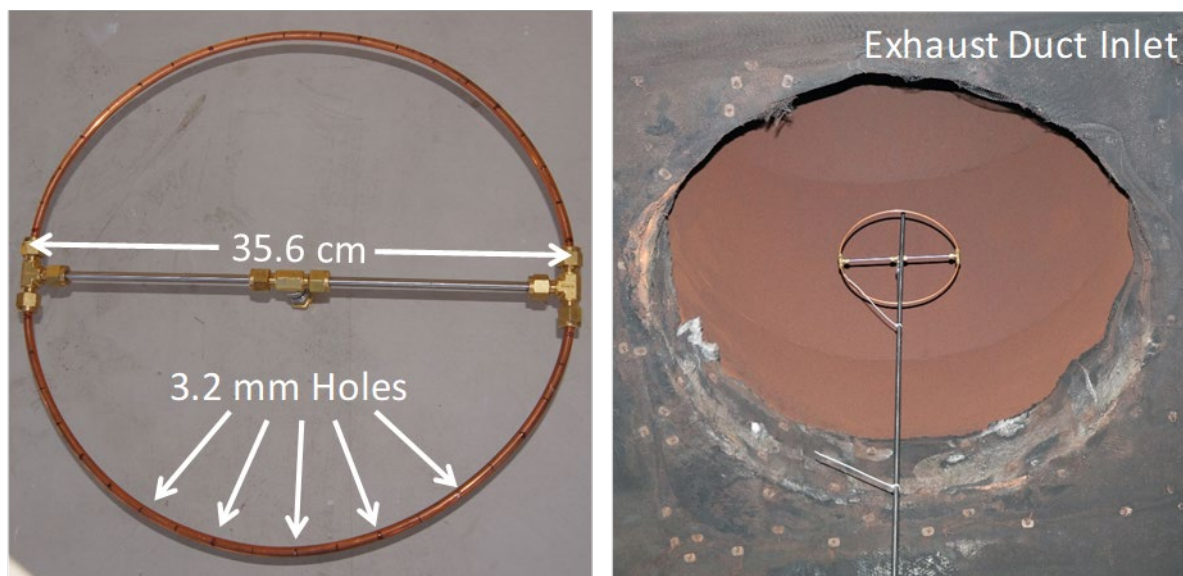


Figure 6 Tracer injection ring (left photo); and injection ring mounted at the inlet of the exhaust duct (right photo).

After the tracer was injected into the exhaust duct, it was mixed and diluted with the entrained air as it traveled through bends in the duct and more than 10 diameters of straight run. At the measurement stations, samples of the diluted tracer gas were continuously drawn from the exhaust duct using the facility’s existing gas sampling and conditioning system. Gas samples were drawn from a stainless-steel tube, mounted horizontally across the exhaust duct, and transported to the gas analyzer, Figure 7. The gas sampling tube has multiple sample ports with 3.2 mm holes drilled every 25.4 cm. Samples collected from the multi-port sampling tube represent the average concentration of tracer across the horizontal chord of the duct.

When conducting fire experiments in the NFRL, it is routine to condition the gas samples before analysis. Conditioning includes filtering to remove particulates and drying to remove water vapor ($< 100 \mu\text{L/L}$ (100 ppmv)). Water vapor was removed using a system of Nafion™ tube dryers (Perma Pure; Model: MG-1228W and PD-200T-72SS). The drying process did not remove SF₆ from the gas sample as confirmed by tests conducted using the calibration mixture. The volume fraction of water vapor in the exhaust gas was measured with a thin film capacitive detector (Vaisala; Model: HMT337) prior to drying the sample. This measurement was used to convert volume fraction measurements to a wet basis.

The gas sample system was assumed to be free of leaks as it had been leak-checked at installation. Leaks in the sample system would bias the flow toward higher values. In general, unusually high flow measurements should be investigated as they could be the result of a leak further diluting the gas sample.

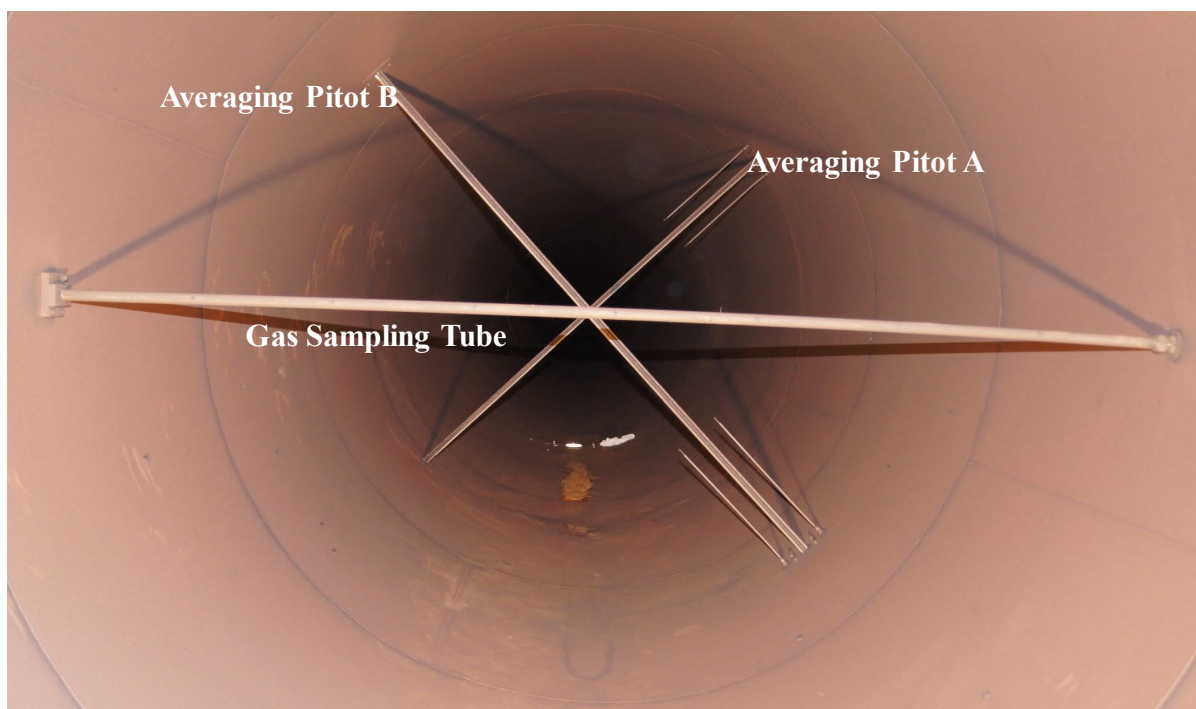


Figure 7 Installation of two averaging pitot probes and the gas sampling tube in the 1.975 m exhaust duct. Photograph view is upstream and into the flow.

A portion of the dry sample was directed to a photoacoustic analyzer (LumaSense Technologies; Model INNOVA 1412i) to measure the diluted volume fraction of SF₆. The analyzer can detect trace amounts of gas in real-time using photoacoustic spectrometry. [20, 21] In this technique, the gas sample is irradiated with infrared light where a portion of the light is absorbed by the gas which then generates an acoustic signal that can be detected by a microphone. The analyzer uses optical filters to select which wavelengths of light irradiate the gas sample and therefore which gases are selected for detection. Sulfur hexafluoride was chosen as the tracer due to its strong absorption in the infrared and very low ambient volume fractions (0.010 nL/L). [22] The disadvantage of using SF₆ as a tracer is it is a greenhouse gas with a high potential for global warming. However, SF₆ is one of a few tracer gases detectable in the range of (0.001 to 100) nL/L that is nontoxic and nonreactive. These features made SF₆ the logical choice for the tracer, since the present study investigated large volume flows, with requirements for generating manageable tracer injection flows, maintaining personal health and safety, and preserving the condition of existing equipment.

Two-point calibrations were performed prior to each experiment using a high-accuracy (calibration) gas mixture to span the photo acoustic analyzer and ultra-high purity (UHP) nitrogen (0.999 99) to zero the analyzer. The span gas had a SF₆ volume fraction of 275 nL/L ± 1 nL/L (275 ppbv ± 1 ppbv) with a balance of dry air. Mixture fraction of the span gas was determined by electron capture gas chromatography. The gas chromatography instrument was calibrated with 5 standard reference materials for mass. In addition, two SF₆ mixtures with volume fractions of 50 nL/L and 100 nL/L were used to confirm the linearity of the photoacoustic analyzer. Manufacturer specifications for the photoacoustic analyzer state a

repeatability of 0.5 % and a detection limit of 6 nL/L for SF₆. This was confirmed using the gas mixtures as stable sources. Cycle time was approximately 40 seconds (0.025 Hz sample rate) for the analyzer measurement. The instrument was capable of shorter cycle times, but the longer measurement duration was chosen to increase measurement precision.

Since water vapor was removed from the sample stream, measurements of gas volume fraction were for a dry gas. To account for the water vapor in the flow, $X_{H_2O,i}$, Eq. (2) was revised to compute the volume flow for the wet conditions in the exhaust duct:

$$\dot{V}_{e,TGD} = \frac{X_{T,I} - X_{T,D}(1 - X_{H_2O,D})}{X_{T,D}(1 - X_{H_2O,D}) - X_{T,U}(1 - X_{H_2O,U})} \dot{V}_{T,I} \quad (8)$$

3.3.1. Optimizing Tracer Injection

Target estimates of injection volume flow for SF₆ were derived using Eq. (2) and the following factors:

- 1) measurement range and detection limit of the photoacoustic analyzer;
- 2) volume fraction of tracer in the gas mixture used to calibrate the photoacoustic analyzer;
- 3) measurement range of the laminar flow element used to monitor the volume flow of the injected tracer;
- 4) operating range of the mass flow controller used to control the injection flow.

Following the guidance of ASTM E2029 [15], injection volume flows were selected to generate diluted volume fractions within ± 20 % of the calibration mixture, solid line in Figure 8. For NFRL's estimated range of exhaust flow, 100 m³/min to 5100 m³/min, a flow metering device capable of delivering up to 1.70 L/min of tracer gas was required to generate the targeted downstream volume fractions. Figure 8 was consulted to determine the optimum injection flow for the desired exhaust flow.

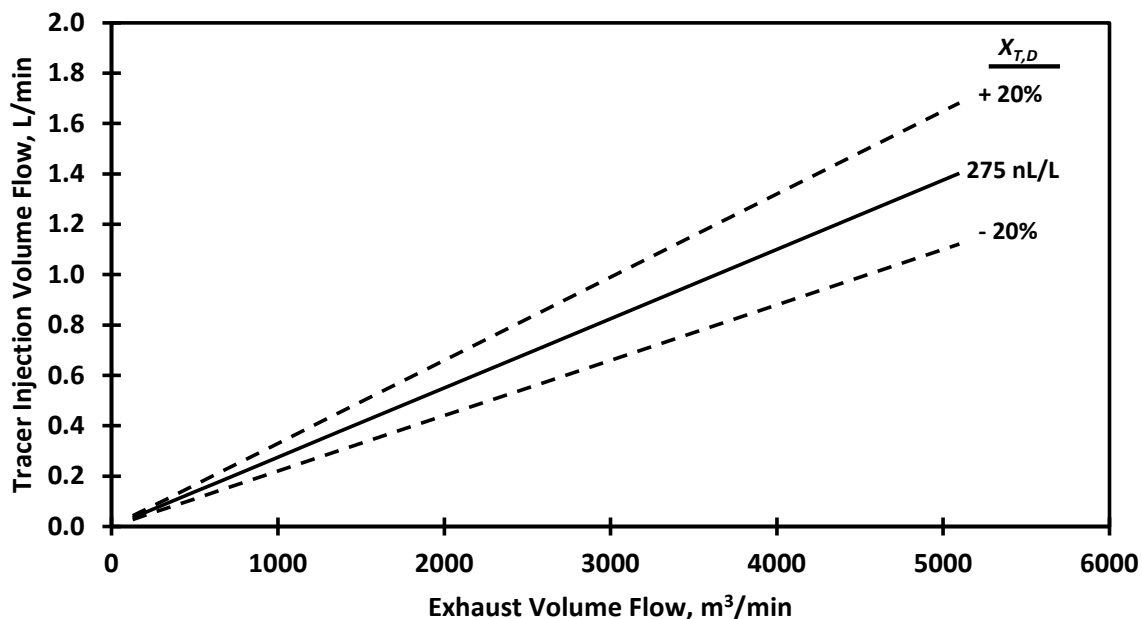


Figure 8 Estimates of tracer injection volume flow required to generate optimal tracer volume fractions downstream. Reference conditions for volume flow are 273.15 K and 101325 Pa.

3.4. Measurement Procedures

Simultaneous measurements of volume flow in the exhaust ducts were conducted using the averaging pitot probes and tracer gas dilution. The following procedures were executed during a typical experiment:

- 1) The exhaust system was initiated, and flow was adjusted to the first target value by monitoring readings from the averaging pitot probes.
- 2) The photoacoustic analyzer was zeroed and spanned (two-point field calibration) with ultra-high purity nitrogen and a high accuracy mixture of SF₆ and dry air, respectively.
- 3) A leak check of the tracer gas injection system was conducted by charging up the system and monitoring volume fraction readings of SF₆ from the photoacoustic analyzer. If no leaks were apparent, the readings served as ambient or upstream measurements of the tracer.
- 4) The tracer injection flow was initiated and adjusted to deliver the optimum amount of tracer for the exhaust flow setting; thus, generating a downstream gas sample with the tracer diluted to volume fractions within the calibration range of the photoacoustic analyzer.
- 5) Volume flow readings from the averaging pitot probes and the tracer gas dilution method were monitored to identify periods of steady experimental conditions. The measurements were continuously logged using NFRL's data acquisition system.
- 6) Once steady conditions for the target flow were achieved, the measurements were tagged for later analysis.

- 7) The exhaust flow was then adjusted to a new target value and, if necessary, the tracer injection flow was adjusted. Conditions were allowed to stabilize, and a new set of readings were tagged for later analysis.

In a typical experiment, measurements were conducted at three to four target values for flow, with repeat measurements at two or more settings. Repeat experiments were conducted on different dates with a minimum of three repeat experiments for each exhaust hood (flow path). Because SF₆ decomposes into toxic compounds at high temperatures, all experiments were conducted without a fire present, using only the ambient air as the exhaust flow. Figure 9 is a time trace of the volume flow measurements and demonstrates a typical calibration experiment. During the periods of steady flow as noted in the figure, the measurements were tagged as being suitable for analysis. Volume flow measurements determined by the TGD method are the average of at least 10 consecutive measurements during steady flow. Because of the slower sample rate of the photoacoustic analyzer, measurements were tagged for a minimum period of 7 minutes.

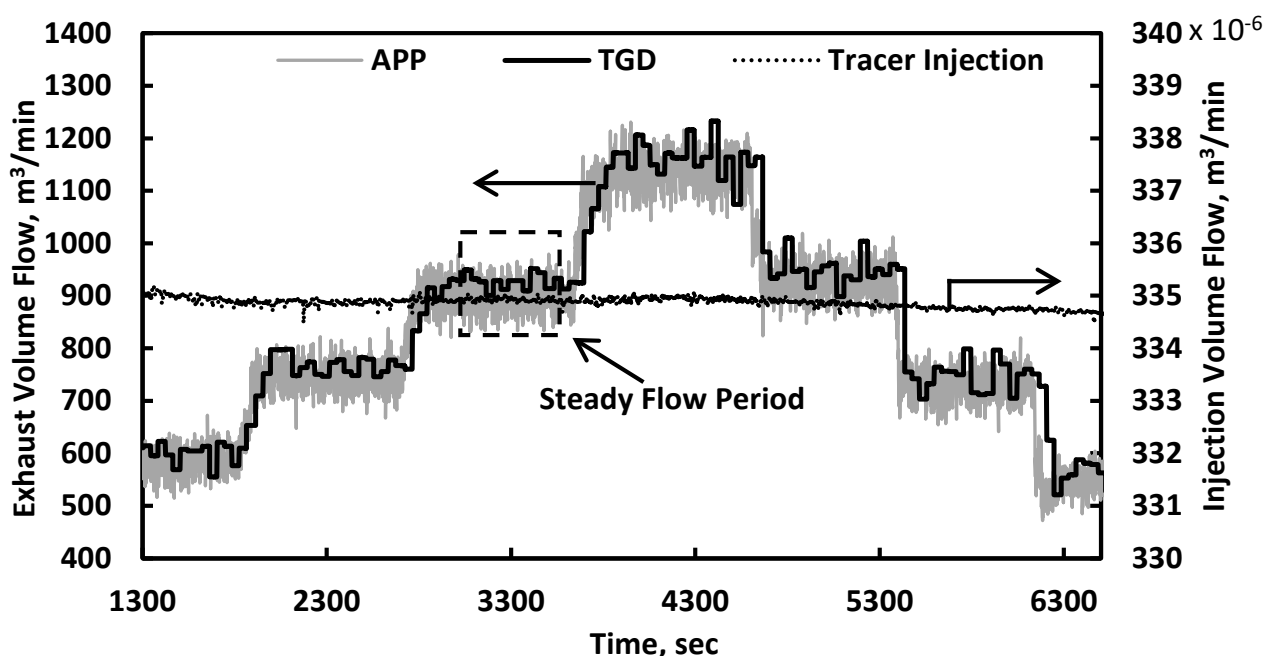


Figure 9 Time trace of a typical experiment. Simultaneous measurements of volume flow using the averaging pitot probes (APP) and the TGD method are shown on the left vertical axis. Volume flow of the injected tracer is shown on the right vertical axis.

4. Results and Discussion

4.1. Measurement Uncertainty – Tracer Gas Dilution

Studies in laboratory-scale ducts and pipes have demonstrated the performance of the constant-injection tracer technique when compared to hot-wire [23, 24], pitot tube [24-26], and turbine flowmeter [27] measurements. Despite the promising performance for field application, only a few studies are available which discuss the constant injection technique in real working ducts

and conduits in the field. [28-30] With the exception of a study of flow through a natural gas compressor [30], the aforementioned studies for ducts and conduits offer little detail on the estimated uncertainty of the tracer gas dilution method. In most cases, only the discrepancy between the tracer gas dilution method and the comparison measurement, usually a pitot tube or hot-wire, is discussed. It is widely known that pitot tube and hot-wire measurements have limited accuracy in duct flows with asymmetric velocity profiles and off-axis flow components due to swirl and turbulence. For this study, tracer gas dilution is the flow calibration method, and therefore a detailed uncertainty analysis of the method is necessary to provide uncertainty estimates for the calibration results.

4.1.1. Test for Sufficient Mixing

The accuracy of the tracer gas dilution method depends on the degree of mixing of the tracer with the transport stream. Sufficient mixing is required to ensure that dilution of the tracer represents the overall flow of the transport gas. ASTM E2029 notes that good practice should result in less than a 10 % variation of tracer concentration across the duct. The standard prescribes a sample traverse at the downstream sample plane and uses the average volume fraction of tracer sampled from a minimum number of locations to determine volume flow. The size of the duct determines the minimum number of sample locations. Averaging the volume fraction for multiple sample locations reduces the impact of mixing on the accuracy of the measurement. Collecting a single sample that is spatially integrated over the sample plane is the physical analog to the sample traverse and its computed average. Collecting a spatially integrated sample can be accomplished with a multi-port sampling tube in less time required to conduct a sample traverse. In the case of less-than-uniform mixing, both methods will generate an average volume fraction, reducing the impact of non-uniformity in the downstream distribution of tracer.

In this study, downstream tracer was collected from a multi-port sampling tube installed in the exhaust duct, as shown in Figure 7, to collect an average tracer concentration and reduce the potential for measurement error. In addition, experiments were conducted to confirm sufficient mixing and the effectiveness of the multi-port sampling. This involved relocating the tracer injection within the inlet plane and conducting repeat experiments. The hypothesis is the downstream distribution of tracer should change with changing injection location if the tracer is un-mixed when it arrives at the downstream sample location. For un-mixed flow, Figure 10 demonstrates that both the single point traverse (SPT) and the multi-port sample (MPT) will provide significantly different results for two different injection locations, Position 1 and Position 2. For the mixed flow, Figure 10 demonstrates that the single point traverse will provide a slightly different volume fraction at each sample location if the tracer is less-than-uniformly mixed. However, for the same condition, a multi-port sample tube will collect a spatially integrated sample, and the resulting volume fraction will be insensitive to small changes in the downstream distribution. Therefore, if there is significant change in downstream volume fraction with relocation of upstream injection location, un-mixed flow at the downstream sample plane is assumed. If there is less than 10 % change in downstream volume fraction with relocation of upstream injection, mixed flow - with less than 10 % variation in tracer distribution, is assumed. In addition, effective compensation for a mixed but less-than-uniform distribution of tracer is assumed in the case of the multi-port sample. The results of this experimental analysis provide a quantitative estimate of the potential measurement error due to mixing.

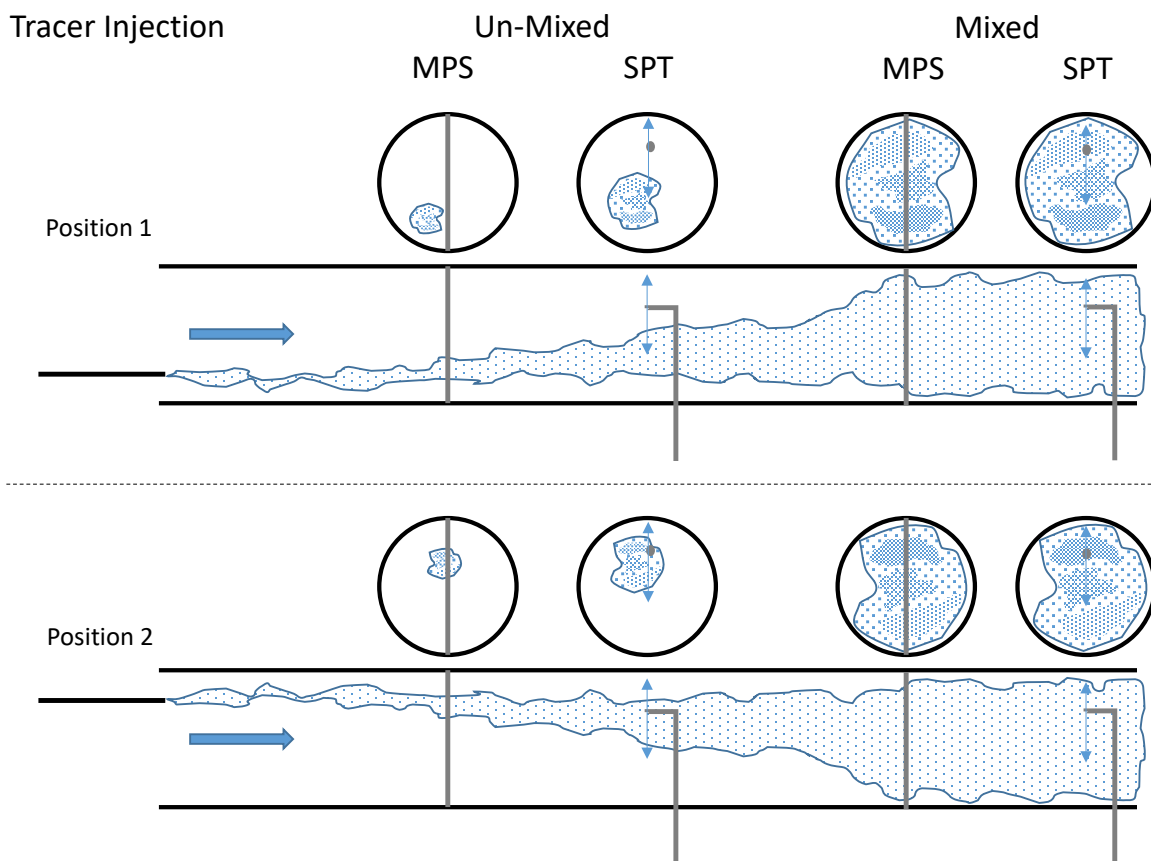


Figure 10 Schematic to demonstrate the impact of injection position of the tracer on the distribution of tracer for downstream locations at un-mixed and mixed conditions, using either a multi-port sample (MPS) or single point traverse (SPT).

Preliminary experiments to test for sufficient mixing were conducted using a single point injection (9.53 mm (ID) stainless steel tube) of tracer at the inlet of the exhaust duct. The exhaust flow and tracer injection rate were held constant while the injection tube was relocated to different quadrants of the injection plane. If the tracer does not completely mix with the flow at the downstream sample location, then any change in the location of the tracer injection should influence the distribution of the tracer at the sample plane downstream as demonstrated in Figure 10. Even though the volume flow is held steady, this would result in an erroneous change in the measured volume flow; especially if the tracer was sampled at a single point. However, a spatially integrated sample, as for the present case, should be insensitive to small changes in the downstream distribution of the tracer, and the resulting volume flow measurement (TGD) should remain steady. This was true as demonstrated by the time trace in Figure 11, which shows a steady volume flow during the period of relocating the tracer injection point.

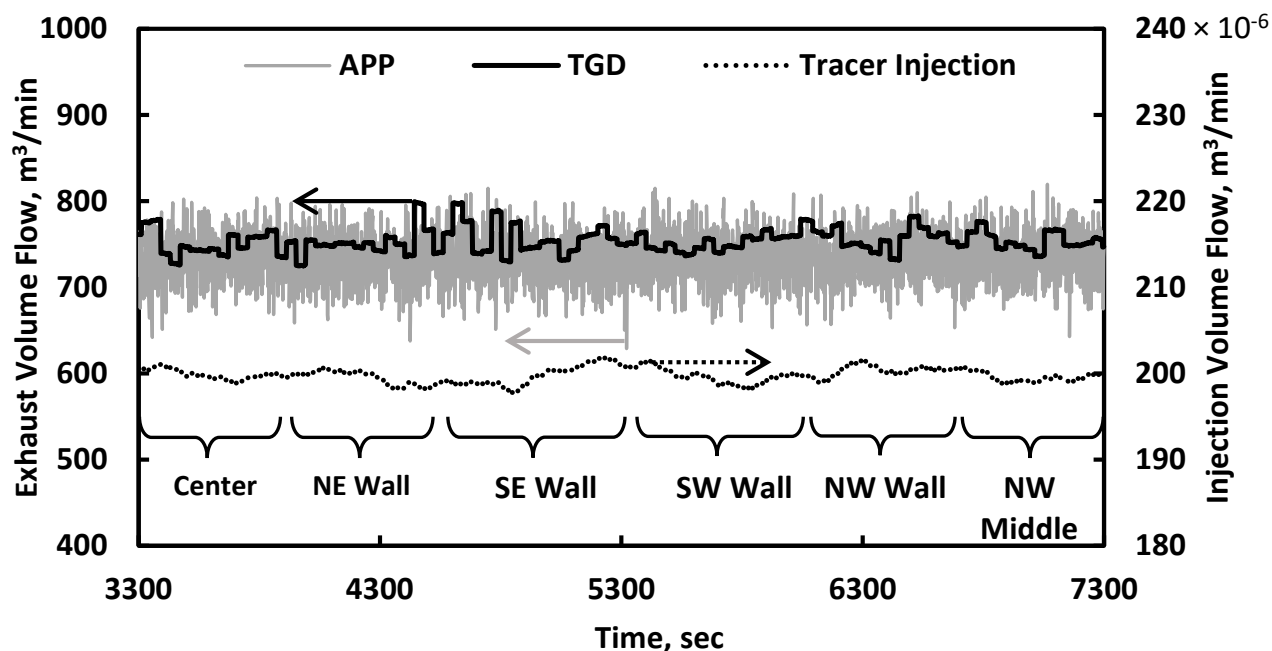


Figure 11 Time trace for a steady exhaust setpoint and tracer injection flow demonstrate TGD providing a steady measurement of exhaust flow during relocation of the tracer injection point at the inlet plane. Brackets indicate location of tracer injection point.

Experiments to test for sufficient mixing were conducted at each calorimeter. For the 3 MW calorimeter, comprehensive measurements were conducted by injecting tracer from a single point, described previously, located at the duct inlet. Flow conditions – exhaust flow and injection flow, were held constant while the location of the injection tube was relocated across the inlet, illustrated in the top-right inset of Figure 12. For this experiment the standard deviation of the volume flow, Figure 12 dashed lines, was less than 0.5 % of the average. The result is consistent with the guidance that one or two bends in a flow path of 10 diameters or more should produce a deviation in the distribution of the tracer across the duct of less than 2 %. [15, 31] The flow path for the 3 MW calorimeter has a straight section of 10 diameters or more and multiple bends upstream of the straight section. Best practices as described by ASTM E2029, usually achieve less than 10 % variation in tracer distribution. [15] The result presented here, which is far less than 10 % variation, suggest that sufficient mixing was achieved. This methodology was used to form a conservative estimate of measurement uncertainty for the TGD method by using the standard deviation of the results from each set of experiments testing for sufficient mixing as a metric of the potential for measurement error due to mixing. Additional details of this experiment are provided in a previous article. [14]

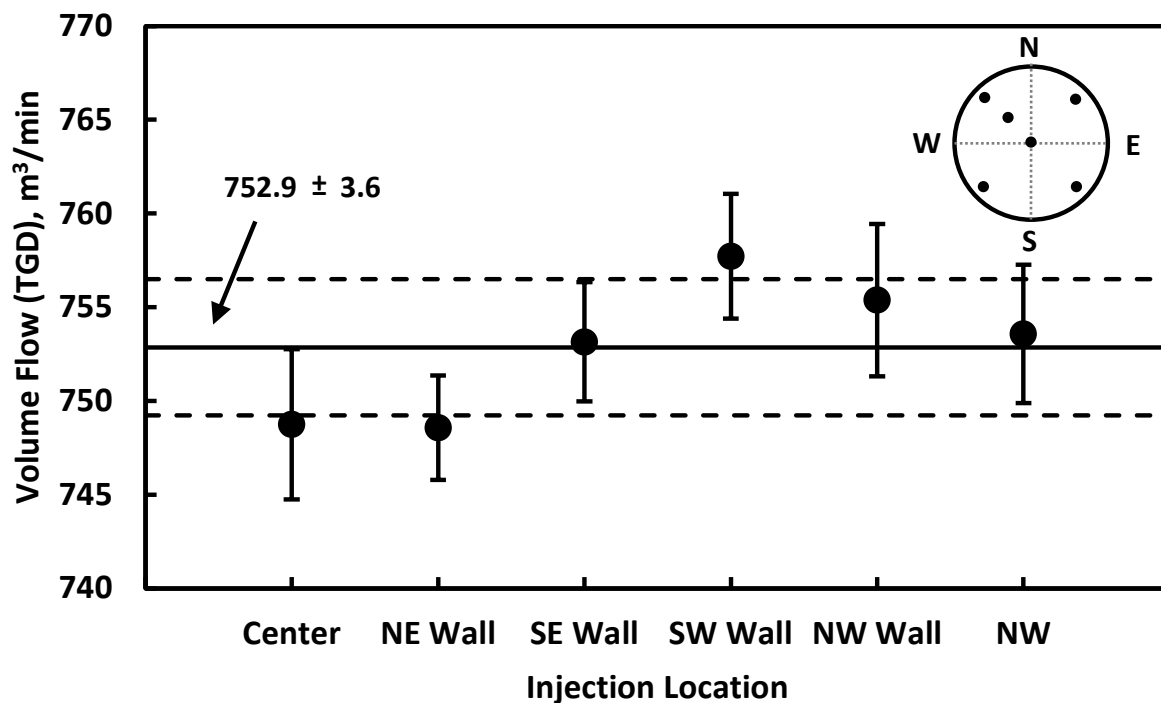


Figure 12 Confirmation of sufficient mixing of the tracer with single point injection for various locations at the exhaust duct inlet. Each point is the mean of 10 or more measurements and the error bars represent the standard deviation of the mean (SDOM). The solid and dashed horizontal lines represent the overall mean and standard deviation, respectively, of the volume flow computed from the 6 locations.

Similar experiments were conducted for the remaining calorimeters to test for sufficient mixing. Tracer was injected only from a single point and from the injector ring for the 0.5 MW calorimeter. For the 10 MW and 20 MW calorimeters, the tracer was injected at various locations along the span of the damper at the hood inlet using the injection ring, Figure 13. Relocation of the injection ring occurred between repeat experiments and included a range of volume flow conditions. The average ratio of the two volume flow measurements, $\dot{V}_{e,TGD}/\dot{V}_{e,APP}$, for each injection location was used to analyze mixing. The standard deviation of this ratio provides the measure for mixing confirmation and the quantitative estimate of the potential error due to mixing, shown in Table 4. This standard deviation was less than 1 % of the average ratio at each of the calorimeters. The result indicates that the error of the volume flow measurement due to the degree of mixing is less than 1 %. Therefore, the spatially integrated gas sample is more than 99 % effective in capturing a gas sample representative of the total flow. Again, this was demonstrated in multiple flow paths of NFRL’s exhaust system.

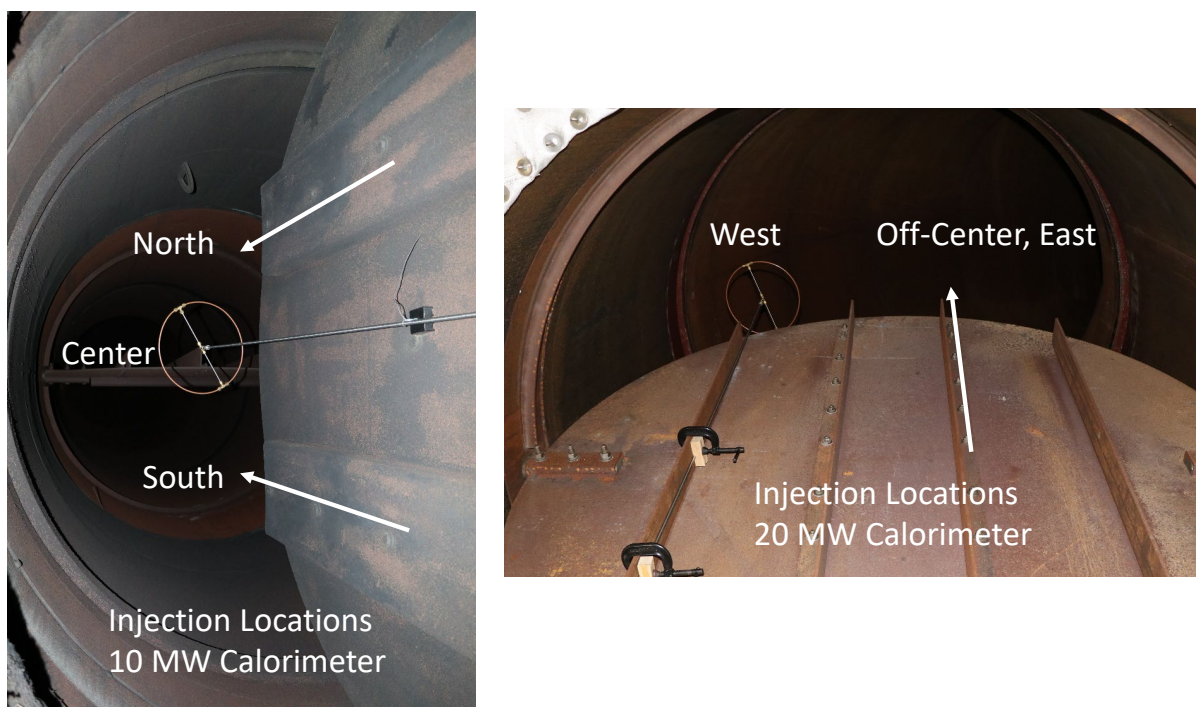


Figure 13 Locations (arrows) of the tracer injection ring for the 10 MW and 20 MW calorimeters.

Table 4 Results of experiments to test for sufficient mixing. The relative standard deviation of the average volume flow ratio across experiments with different injection locations provides an estimate of the potential for measurement error due to inadequate mixing.

Calorimeter	Relative Standard Deviation $\sigma_{\text{ratio}} / \left(\dot{V}_{e,\text{TGD}} / \dot{V}_{e,\text{APP}} \right)$	Injector; Location (No. of Repeats)
0.5 MW	0.006	Ring; Center (1) Point; Center (2), Northwest (2)
3.0 MW	0.006	Point; Center (1), Northeast (1), Southeast (1), Southwest (1), Northwest (2)
10 MW	0.007	Ring; Center (3), North (1), South (1)
20 MW	0.006	Ring; Off-Center East (2), West (2)

Less than 1% measurement error due to mixing for these experiments is significant. It validates that the experimental configuration and procedures surpasses the suggested best practices of ASTM E2029, the standard method for the tracer gas volume flow measurement.

It also validates the effectiveness of the spatially integrated gas sample (multi-port sample tube) and demonstrates that it can be used as an alternative to single point sample traverses.

The experiments also demonstrate how to evaluate the performance of gas species measurements for oxygen consumption calorimetry. These experiments are analogous to small fires in large ventilation hoods with exhaust flow large enough to rapidly transport the plume into the duct, not allowing it to fill the hood. In most practical cases the fire will be large enough to generate a plume that partially fills the hood. In such cases, the plume will experience additional mixing before entering the exhaust inlet with flow turnover in the canopy hood. Hence the results of this study can be used to estimate an upper limit on the error due to mixing in the species concentration measurements for calorimetry or other studies.

4.1.2. Estimated Uncertainty

A detailed analysis to estimate the uncertainty of the volume flow measurements using the TGD method has been described in a previous article. [14] The analysis was applied for the volume flow measurements at each of NFRL's calorimeters. This analysis is demonstrated in Appendix B with a detailed uncertainty budget for volume flow measurements at the 3 MW calorimeter. Estimates for the relative expanded uncertainty were 0.03, on average, as shown in Figure 14 and Figure 15. The uncertainty estimates apply for flows ranging from 90 m³/min to 5400 m³/min (mass flows ranging from 1.9 kg/s to 116 kg/s); spanning the routine operating conditions for NFRL's calorimeters. Figure 15 shows that the uncertainty of the exhaust flow measured at the 20 MW calorimeter increased significantly for flows less than 1200 m³/min. For large fire experiments requiring exhaust flows less than 1200 m³/min, the 10 MW and 3 MW calorimeters are recommended. The 20 MW calorimeter is part of the expansion of NFRL's existing calorimetry system and one of the largest calorimeters in existence for the study of large fires. Investigations such as this are necessary to provide detailed characterizations of unique measurement systems. These investigations also document a measurement system's capabilities and limitations as well as provide insight on how to optimize the measurement performance of the system.

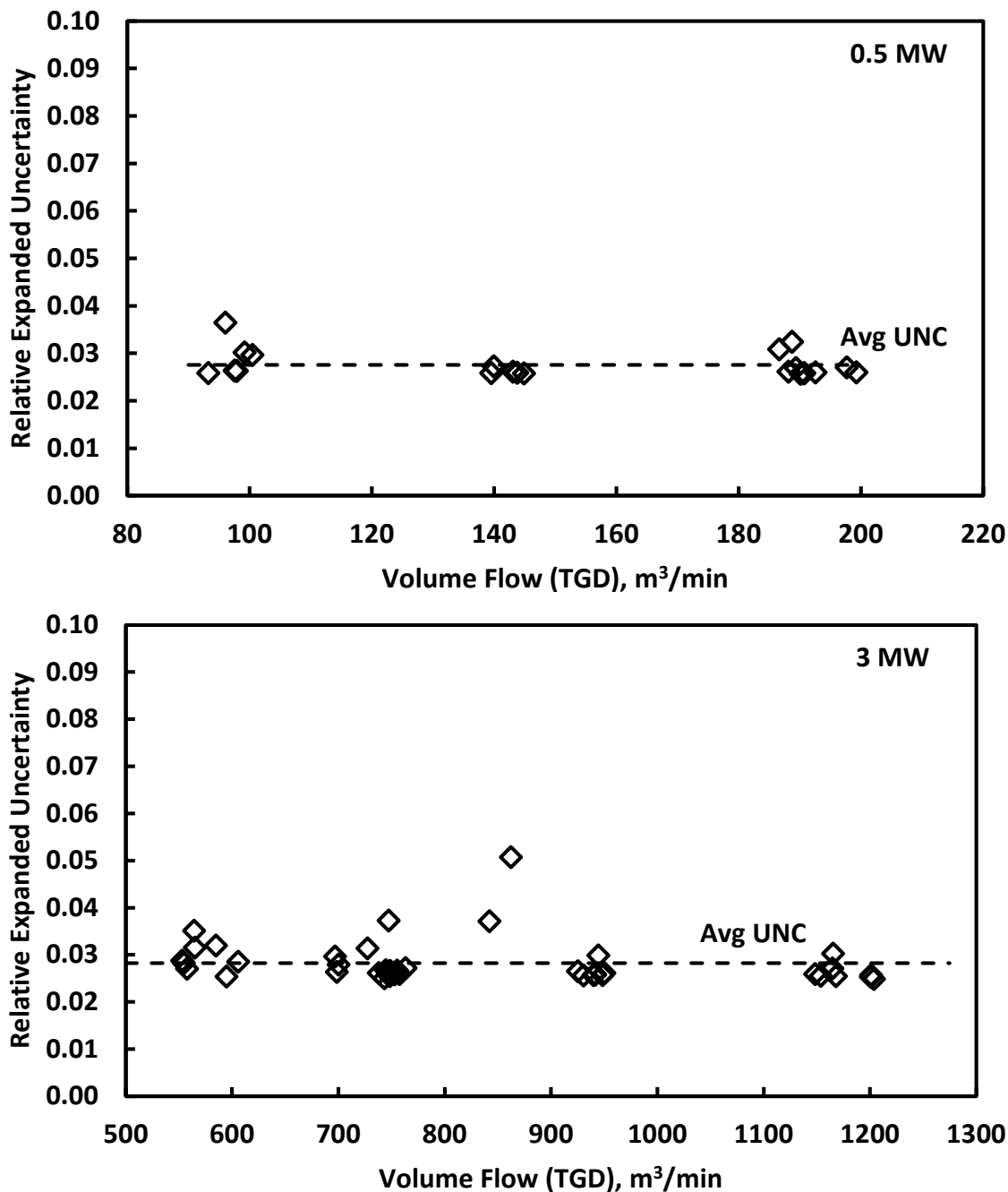


Figure 14 Measurement uncertainty estimates of volume flow determined using TGD at the exhaust ducts of the 0.5 MW and 3 MW calorimeters. The dashed line represents the average uncertainty for the range of volume flow during routine operations.

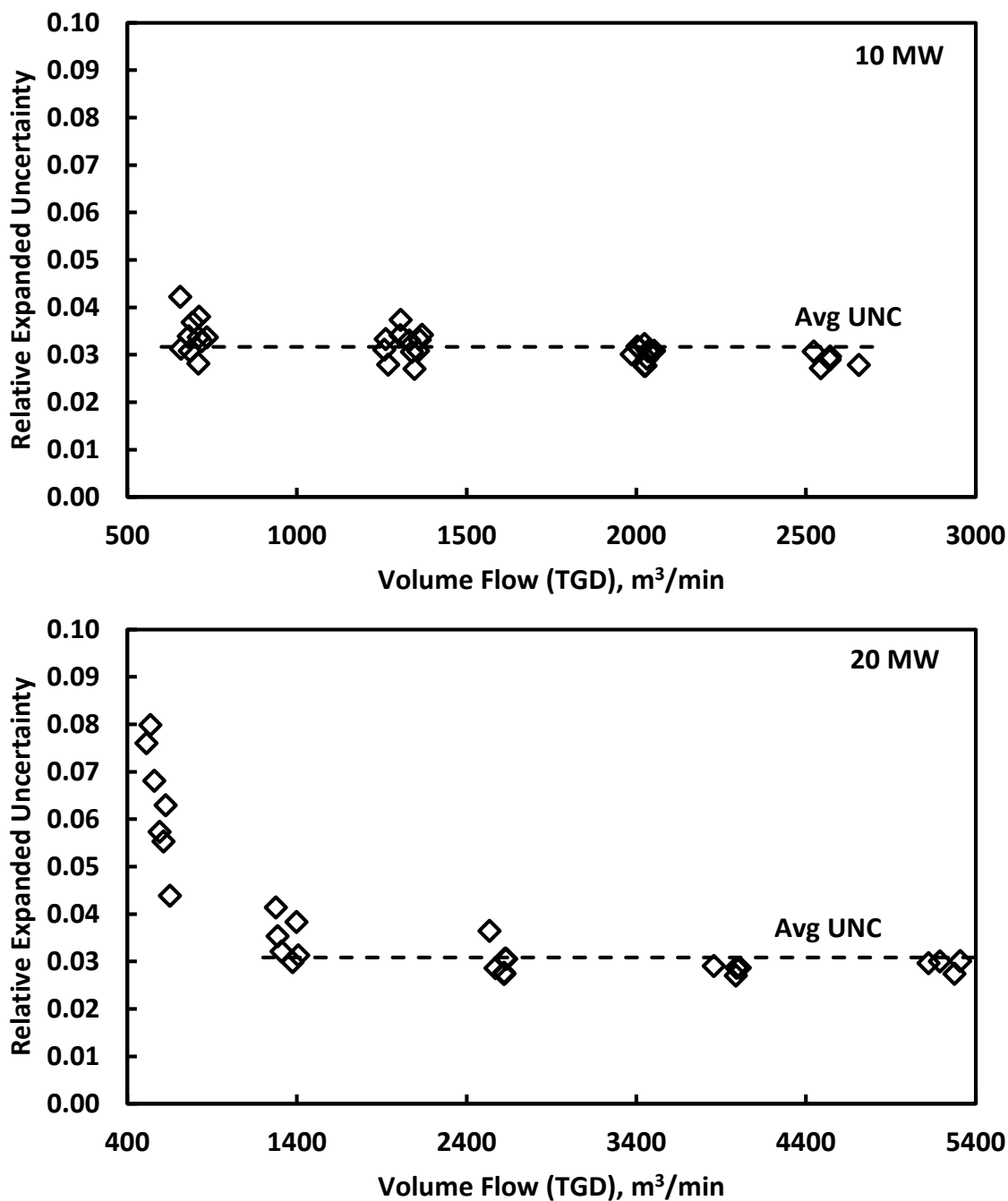


Figure 15 Measurement uncertainty estimates of volume flow determined using TGD at the exhaust ducts of the 10 MW and 20 MW calorimeters. The dashed line represents the average uncertainty for the range of volume flow during routine operations (Lower limit is 1200 m³/min for the 20 MW calorimeter).

Table 5 summarizes the estimated measurement uncertainty for the volume flow measurements using TGD. For the experiments described here, three major contributors to the measurement uncertainty were identified: the measurement of downstream tracer volume fraction (tracer detection at the photoacoustic analyzer), measurement repeatability (standard deviation of the mean - SDOM), and error due to inadequate mixing. The measurement for downstream tracer volume fraction accounts for over 50 % of the combined uncertainty. The contribution from measurement repeatability ranges from 10 % to 30 %, and the contribution from the error due to inadequate mixing ranges from 12 % to 21 %. The volume flow measurement of the injected tracer has the potential to be a major contributor, therefore it is also listed in Table 5. Its contribution will be greater when utilizing flow monitoring devices with lower accuracy (rotameters or standard mass flow controllers) for tracer injection. For this study the contribution to uncertainty was small due to the use of a laminar flow element with low measurement uncertainty.

Table 5 Estimated uncertainty for measurements of volume flow in the NFRL exhaust system using tracer gas dilution.

Measurement Component, x_i	0.5 MW		3.0 MW		10 MW		20 MW	
	$u(x_i)/x_i$	~%*	$u(x_i)/x_i$	~%*	$u(x_i)/x_i$	~%*	$u(x_i)/x_i$	~%*
Downstream Tracer								
Volume Fraction, $X_{T,D}$	0.011	70	0.011	68	0.011	53	0.011	55
Injected Tracer								
Volume Flow, $\dot{V}_{T,I}$	0.0007	<1	0.0007	<1	0.0007	<1	0.0007	<1
Repeatability (SDOM)	0.004	9	0.006	20	0.008	27	0.008	28
Error Due to Inadequate Mixing	0.006	21	0.005	12	0.007	20	0.006	17
Standard, $u_c(y)/y$	0.013		0.014		0.016		0.015	
Expanded, $U(y)/y$	0.027		0.028		0.032		0.031	

*Percent contribution (rounded approximation) of the component uncertainty to the combined standard uncertainty.

The repeatability of the volume flow measurement as well as the measurement error due to mixing will depend on factors such as the design of the experiment, instrumentation, flow configurations, and flow conditions. Each can contribute more than 10 % to the combined uncertainty, and hence their impact on the measurement uncertainty should be evaluated before

proceeding with an experimental test series. For example, insufficient mixing can lead to significant measurement error. Multiple locations for tracer injection or passive devices to enhance mixing are typical methods to reduce the potential for measurement error. As demonstrated, distributed injection (injection ring) combined with simultaneous sampling from multiple locations (multi-port sample tube) in the downstream sample plane and screening experiments to confirm sufficient mixing are effective methods to reduce the uncertainty due to tracer mixing.

The reader should note that the uncertainty estimates presented apply to the specific setup of the TGD method and for the flow conditions and exhaust duct configuration of the NFRL. The results may not generally apply to other experimental setups and flow configurations, as each large-scale fire facility or flue exhaust system is unique. It is the responsibility of the experimentalist to determine the measurement uncertainty for their test conditions.

4.2. In-Line Calibration of Averaging Pitot Probes

Flow coefficients (K_a) are provided for the averaging pitot probes by the manufacturer, as shown in Table 2. The coefficients are most accurate for a turbulent and fully-developed pipe flow, therefore a flow that is symmetrical in all directions across the pipe. A flow profile that is asymmetric due to upstream disturbances will introduce error in the flow measurement. If asymmetry exists, an in-line calibration of the probe is recommended to correct the flow measurement and improve accuracy. For NFRL's exhaust ducts, more than 10 diameters of straight run exist upstream of each flow measurement location to allow the flow to develop a favorable distribution at the measurement station. Flow conditioning methods, such as screens, straightening tubes, or disturbance plates, have not been implemented. For some flow cases the averaging pitot probes (A and B), installed as shown in 4, did not measure the same gas velocity. Whenever the ratio of the velocity, $V_{e,A}/V_{e,B}$, deviates from unity, asymmetric flow is suspected as discussed in a previous article. [13] Therefore an in-line calibration of the probes was conducted using tracer gas dilution, which provides an independent measurement of volume flow as determined by comparing Eq. (7) and Eq. (8).

Calibration experiments were conducted following the procedures described in Section 3.4. An experiment consisted of 3 to 4 flow settings that targeted approximately 10 % to 25 %, 50 %, 75 %, and 100 % of the flow capacity at each calorimeter. A minimum of 3 repeat experiments were conducted for each calorimeter with repeats occurring on separate days. Up to 7 repeats were conducted for the 3 MW calorimeter as it was used to initially evaluate the error due to flow mixing for the tracer gas dilution measurement.

The results of the calibration experiments are shown in Figure 16 and Figure 17. For the NFRL exhaust ducts, the ratio of volume flow is greater than unity, meaning the volume flow measured with the averaging pitot probes consistently underestimates that determined by TGD. This is consistent with previous comparisons for measurements of heat release rate by oxygen consumption calorimetry and the theoretical output from a natural gas burner (fuel consumption calorimetry) made prior to the flow calibration. Those comparisons demonstrated the oxygen consumption calorimetry measurements, which are proportional to exhaust flow, consistently under predicting the theoretical output from a natural gas burner. The heat release comparison provided more evidence of the need for an in-line calibration. [13]

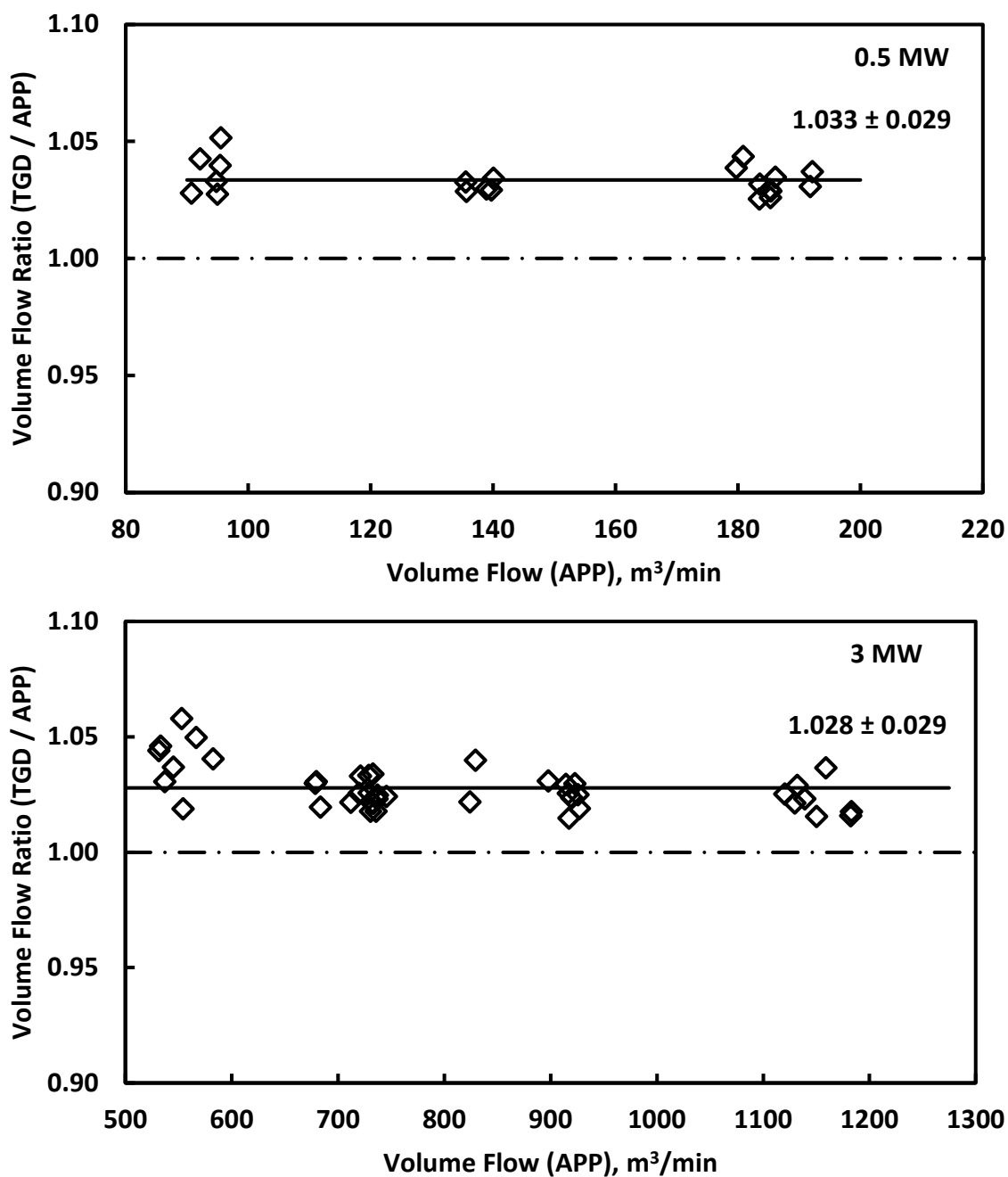


Figure 16 Results of flow calibration experiments at the 0.5 MW and 3 MW calorimeters. The ratio of volume flow measured using tracer gas dilution and averaging pitot probes are shown. The solid line represents the average ratio over the operational range of flow for each calorimeter.

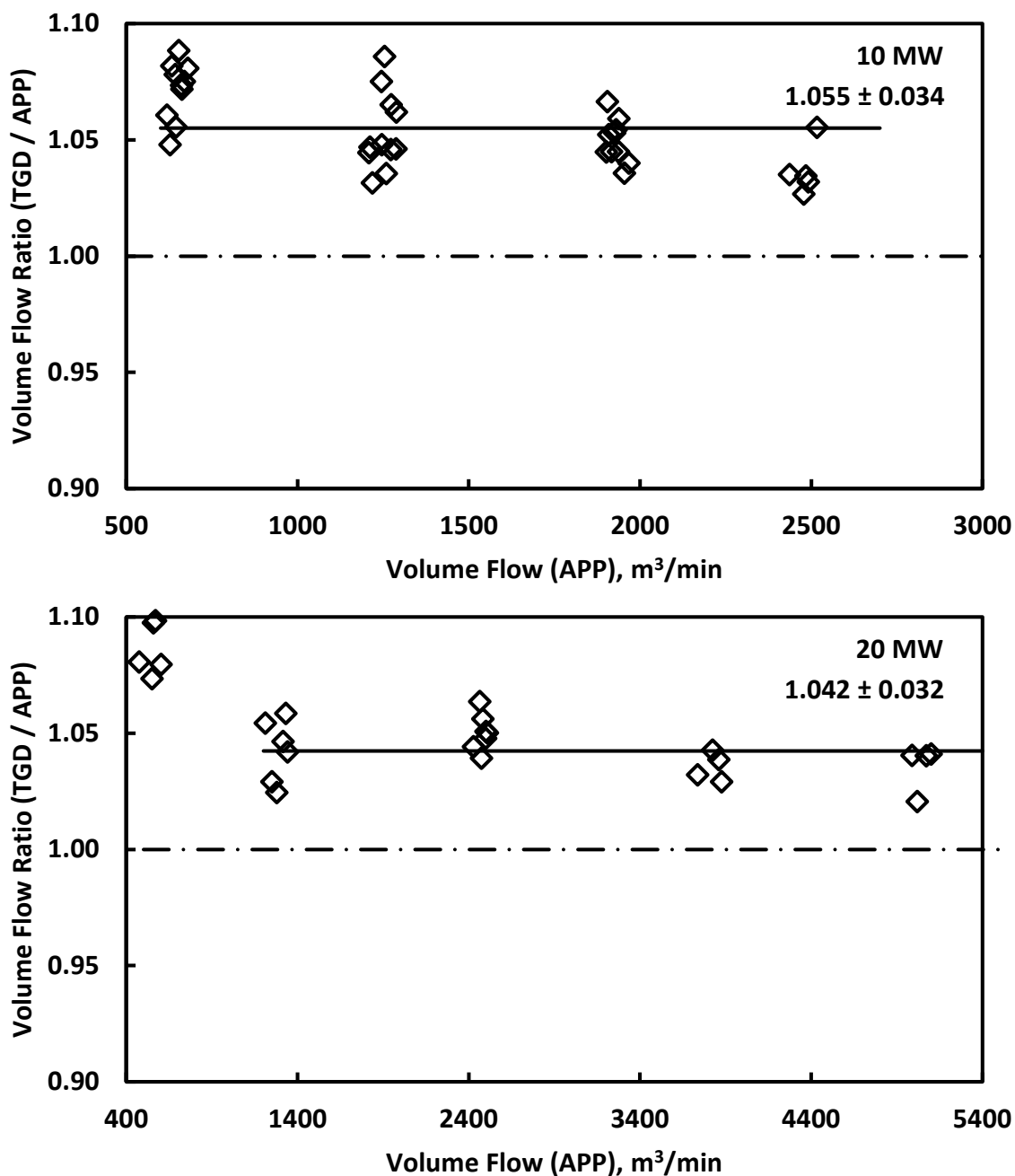


Figure 17 Results of flow calibration experiments at the 10 MW and 20 MW calorimeters. The ratio of volume flow measured using tracer gas dilution and averaging pitot probes are shown. The solid line represents the average ratio over the operational range of flow for each calorimeter.

Across the operational flow range of each calorimeter, Figure 16 and Figure 17 show flow ratio as essentially constant. The calibration constant, C_f , for flow is therefore computed as the average ratio of volume flow, Eq. (9).

$$C_f = \frac{1}{N} \sum \left(\frac{\dot{V}_{e,TGD}}{\dot{V}_{e,APP}} \right) \quad (9)$$

This correction is applied to flow measurements determined by the averaging pitot probes for each calorimeter. Flow calibration constants for each calorimeter (or exhaust flow path) are listed in Table 6 along with estimates of expanded uncertainty. These estimates include the uncertainty of the TGD method. Using the calibration constant, an effective exhaust velocity, Eq. (10), or better determination of total flow is achieved. Correcting the flow measurements with the in-line calibration improved measurement accuracy for the range of flows listed. The uncertainty of the calibration increases for flows outside of the range.

$$V_{e,eff} = C_f V_{e,avg} \quad (10)$$

Recall the tracer gas dilution method is a volumetric, or whole field, method for measuring flow that is independent of the averaging pitot probes. Because it is not sensitive to flow asymmetry, it is well suited for the in-line calibration of large-scale flows utilizing averaging pitot probes.

Table 6 Flow calibration constants determined from the in-line calibration of the averaging pitot probes using tracer gas dilution.

Calorimeter	Flow Calibration Constant, C_f	Flow Range
0.5 MW	1.033 ± 0.029	(90 to 200) m ³ /min* (1.9 to 4.3) kg/s
3 MW	1.028 ± 0.029	(500 to 1275) m ³ /min* (10.8 to 27.5) kg/s
10 MW	1.055 ± 0.034	(600 to 2700) m ³ /min* (12.9 to 58.2) kg/s
20 MW	1.042 ± 0.032	(1200 to 5400) m ³ /min* (25.9 to 116) kg/s

*Reference conditions for volume flow are 273.15 K and 101325 Pa.

The results of Figure 16, Figure 17, and Table 6 show that measurements from the averaging pitot probes under-estimate the volume flow at NFRL's exhaust ducts by 3 % to 6 %. Major fire test standards (ASTM, ISO) for large fire calorimetry state accuracy requirements for flow measurements at 5 % to 6 %. [8, 9, 32] The under-estimate does not exceed the stated accuracy requirements for flow, therefore NFRL's exhaust flow measurements would still be in

compliance with these standards without the flow calibration as demonstrated in a previous publication. [13] However, achieving the best accuracy while advancing the state-of-the-art for large-scale calorimetry is the purpose of this study.

Some fire test standards recommend using the difference in heat release rate between burner and calorimetry as the flow correction factor or overall correction factor for the oxygen consumption calorimetry measurement. In-line or in-situ calibrations of flow devices is best practice when feasible. A system correction based on a comparison of calorimetry measurements is a practical solution but not the best practice to improve accuracy. It is well known that flow conditions play an important role in the performance of calorimetry measurements using oxygen consumption. [33] If flow conditions are not well characterized and reproduceable, corrections based on burner outputs may not be reliable. The in-line flow calibration is more robust since it is valid for a range of flow conditions and decouples errors due to plume capture and measurement of fuel consumption from the calorimetry measurement.

4.2.1. Calibrated Exhaust Flow Measurements

Heat release may be computed based on mass instead of volume as describe by Eq. (1). NFRL's computation of heat release, Eq. (11), is based on mass and includes measurements of additional gases – carbon monoxide (X_{CO}), carbon dioxide (X_{CO_2}), and water (X_{H_2O}), to improve the accuracy of the computation. Mass flow through the exhaust duct, \dot{m}_e , is the required measurement. It is inferred from the velocity measurement at each averaging pitot probe and combined to provide an average mass flow. The flow calibration constants determined from the in-line calibration are applied to achieve better measurement accuracy for exhaust mass flow, as shown in Eq. (12). Time history measurements of the calibrated exhaust mass flow are presented in Figure 18.

$$\dot{Q}_{OC} = \left[(\Delta_c H_{fuel})_{O_2} \phi - ((\Delta_c H_{CO})_{O_2} - (\Delta_c H_{fuel})_{O_2}) \frac{1-\phi}{2} \frac{X_{CO}}{X_{O_2}} \right] \frac{\dot{m}_{e,eff}}{1+\phi(\alpha-1)} (1 - X_{H_2O}^o) X_{O_2}^o \frac{M_{O_2}}{M_{air}} \quad (11)$$

$$\dot{m}_{e,eff} = C_f \left(\frac{\dot{m}_{e,A} + \dot{m}_{e,B}}{2} \right) \quad (12)$$

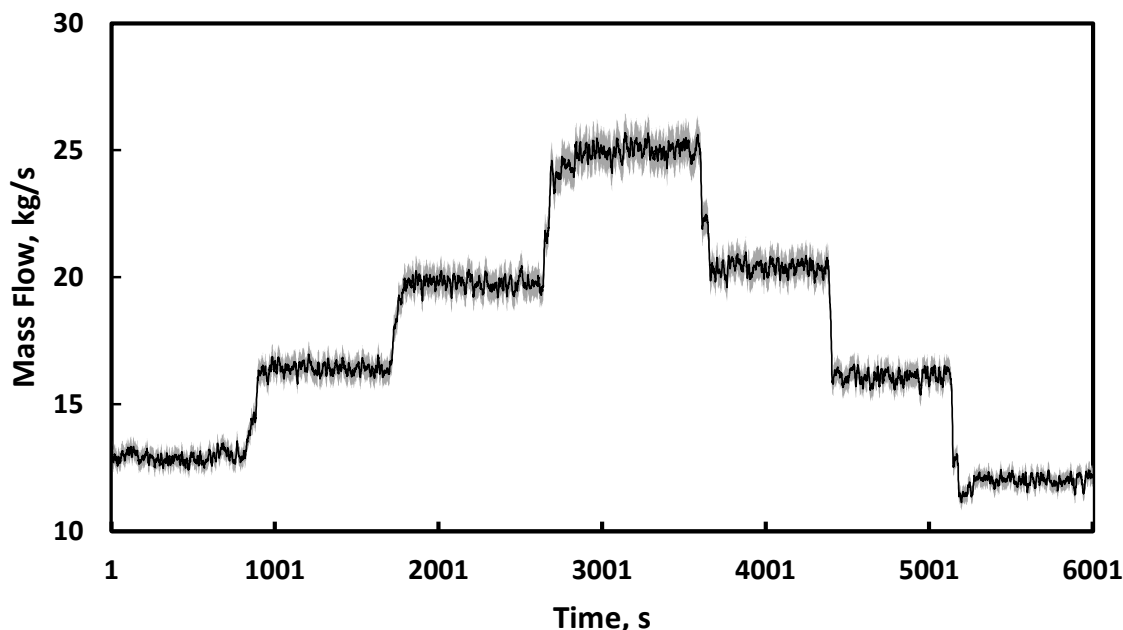


Figure 18 Calibrated mass flow for the 3 MW calorimeter. Shaded region represents the estimated expanded uncertainty.

Estimates of measurement uncertainty for calibrated exhaust velocity and mass flow are presented in Table 7 for each of the calorimeters. The expanded uncertainty of the gas flow measurement is approximately 3 % at each calorimeter. The uncertainty estimates are valid for the flow ranges listed in Table 6. Since mass flow is derived from the gas velocity measurement, its expanded uncertainty is slightly increased, but still approximately 3 %. The slight increase is most apparent for the 0.5 MW calorimeter due to contribution from uncertainty of the effective duct diameter.

Four parameters, C_f , K_a , D_{eff} , and M_{air} , contribute more than 98% uncertainty to the mass flow measurement, while 3 of the 4 parameters, C_f , K_a , and M_{air} , contribute more than 98 % uncertainty to the measurement of effective gas velocity. The uncertainty contributions from these four parameters only are presented in Table 7 for brevity. In all cases, uncertainty from the flow calibration constant, C_f , dominates. It contributes more than 90 % to the combined uncertainty of the gas velocity measurement, and more than 70 % to the combined uncertainty of mass flow. Due to low measurement uncertainty for the differential pressure and gas temperature measurements, their contribution is on the order of 1 % to 2 %. This is demonstrated in the detailed uncertainty budgets presented in Appendix B. Because the uncertainty of the mass flow measurement contributes significantly to the measurement uncertainty of heat release rate, considerable attention was devoted to accurately determining C_f as discussed here and D_{eff} , as discussed in previous publications. [12, 13]

Table 7 Estimated uncertainty for flow measurements in the NFRL exhaust system using the averaging pitot probes.

Measurement Component, x_i	0.5 MW		3 MW		10 MW		20 MW	
	$u(x_i)/x_i$	$\sim\%*$ $\dot{m}_{e,eff}$ ($V_{e,eff}$)						
C_f (-)	0.014	71 (91)	0.014	88 (91)	0.016	91 (93)	0.015	88 (92)
K_a (-)	0.0038	5 (7)	0.0038	6 (6)	0.0038	5 (5)	0.0038	5 (6)
D_{eff} (m)	0.004	22 (-)	0.0013	3 (-)	0.0013	2 (-)	0.0019	5 (-)
M_{air} (kg /kmol)	0.0035	1 (1)	0.0035	1 (1)	0.0035	1 (1)	0.0035	1 (1)
Standard, $u_c(y)/y$	0.017 (0.015)		0.015 (0.015)		0.017 (0.017)		0.016 (0.016)	
Expanded, $U(y)/y$	0.034 (0.030)		0.030 (0.030)		0.034 (0.034)		0.032 (0.032)	

*Percent contribution (rounded approximation) of the component uncertainty to the combined standard uncertainty.

5. Summary

Exhaust flow measurements have long been identified as a significant source of error for large-scale calorimetry. Averaging pitot probes have been installed at NFRL’s exhaust ducts to improve the exhaust flow measurements and hence improve NFRL’s capability to provide accurate measurements for oxygen consumption calorimetry. Averaging pitot probes are widely used for monitoring large-scale flows in many industries, but their accuracy depends on installation and the flow profile under investigation. Previous flow studies at NFRL exhaust ducts provided data that suggest asymmetric flow. To improve their accuracy, an in-line calibration of the averaging pitot probes was conducted using tracer gas dilution as a reference flow measurement.

ASTM E2029 is the standard test method for determining volume flow in ducts using tracer gas dilution. It is a volumetric, or whole field, method that is not sensitive to asymmetric flow distributions. It is also independent of measurement methods using pressure impact probes (pitot probes) to determine flow. Therefore, tracer gas dilution is an ideal candidate for in-line calibrations of flow measurement devices in large conduits. For the first time, tracer gas dilution has been demonstrated as a calibration method for the exhaust flow measurements essential to large fire calorimetry. The averaging pitot probes at each of NFRL’s four calorimeters have been calibrated using this independent technique. Measurement uncertainty for the calibration is estimated at 3 % and includes estimates for error due to inadequate mixing

of the tracer. The accuracy of the tracer gas dilution measurement depends on how well the tracer is mixed in the transport stream. In the case of non-uniform mixing, a spatially integrated gas sample can be drawn to average any non-uniformity in the distribution of the tracer. A multi-port sampling tube was used to extract a spatially integrated gas sample and therefore reduce potential bias error caused by a non-uniform distribution of tracer.

Experiments were conducted to confirm sufficient mixing of the tracer and the effectiveness of the multi-port sampling tube. The potential bias error due to mixing was less than 1 % for the volume flow measurements determined by tracer gas dilution. Therefore, use of the multi-port sample tube was more than 99 % effective in capturing a gas sample representative of total flow. Less than 1 % measurement error due to inadequate mixing for such large-scale flows is significant. It validates that the experimental configuration and procedures surpass the requirements of the ASTM standard (E2029). It also demonstrates that spatially integrated gas sampling techniques such as the multi-port sample tube are as effective as single point sample traverses and can serve as an alternative sampling strategy. In addition, the results of this study can serve as an estimate for the upper limits of error due to inadequate mixing for the species concentration measurements used for calorimetry or other studies in the NFRL.

The results provided flow calibration constants for each calorimeter. The calibration constants ranged from 1.03 to 1.06, showing consistent under-prediction of total flow by the averaging pitot probes. Application of the flow calibration constants provide more accurate measurements of exhaust gas velocity and exhaust mass flow, necessary inputs for computed values such as heat release rate. Measurement uncertainty for the effective (corrected) gas velocity and mass flow is estimated at 3 %. The in-line calibration of the exhaust flow measurement replaces the common practice of correcting the flow measurement based on the comparison with a known heat release from a gas burner as described by some fire test standards. This practice couples any error in determining heat content and fuel flow at the burner with that of the calorimeter. It is a practical solution but not the best practice to improve accuracy. Conducting an in-situ calibration of the flow measurement device as demonstrated here is best practice. The in-line flow calibration is valid for a wide range of flow conditions and is therefore more robust. Most important, it decouples measurement error between oxygen consumption calorimetry and fuel consumption calorimetry allowing for an independent confirmation of the two calorimetry methods.

Acknowledgments

The author gratefully acknowledges the technical and engineering support provided by Matt Bundy, NFRL Director; Laurean DeLauter, Doris Rinehart and Anthony Chakalis, NFRL Technicians. The author is most grateful to Artur Chernovsky, NFRL Electronics Engineer, for developing data acquisition and control applications; to John Wright of the Fluid Metrology Group for use of the laminar flow element; and to George Rhoderick of the Gas Sensing Metrology Group for analysis of the calibration mixtures. Research support by the Greenhouse Gas Measurements Program, James Whetstone, Program Manager, NIST Special Programs Office, is gratefully acknowledged.

References

- [1] Janssens ML (2002) Calorimetry. *The SFPE Handbook of Fire Protection Engineering*, ed DiNenno PD, D; Beyler, CL; Walton, WD; Custer, RLP; Hall, JR; Watts, JM (National Fire Protection Association, Quincy, MA), Chapter 2, 3rd Ed., pp Section 3:38-62.
- [2] Yeager RW (1986) Uncertainty Analysis of Energy-Release Rate Measurement for Room Fires. *Journal of Fire Sciences* 4(4):276-296.
- [3] Enright PA , Fleischmann CM (1999) Uncertainty of heat release rate calculation of the ISO5660-1 cone calorimeter standard test method. *Fire Technology* 35(2):153-169.
- [4] Axelsson J, Andersson P, Lonnermark A, VanHees P, Wetterlund I (2001) Uncertainties in Measuring Heat and Smoke Release Rates in the Room/Corner Test and the SBI. (Boras, Sweden), SP Report 2001:04, 2001.
- [5] Brohez S (2005) Uncertainty analysis of heat release rate measurement from oxygen consumption calorimetry. *Fire and Materials* 29(6):383-394.
- [6] Sette B (2005) Evaluation of Uncertainty and Improvement of the Single Burning Item Test Method. (Ph.D. Thesis, University of Ghent, Belgium).
- [7] Bryant RA , Mulholland GW (2008) A guide to characterizing heat release rate measurement uncertainty for full-scale fire tests. *Fire and Materials* 32(3):121-139. <https://doi.org/10.1002/fam.959>
- [8] ASTM (2015) Standard Practice for Full-Scale Oxygen Consumption Calorimetry Fire Tests. (ASTM International, West Conshohocken, PA), ASTM E 2067-15.
- [9] ISO (2008) Fire Tests - Open Calorimetry - Measurement of the Rate of Production of Heat and Combustion Products for Fires of up to 40 MW. (International Organization for Standardization, Switzerland), ISO 24473:2008(E).
- [10] ASTM (2016) Standard Test Method for Heat and Visible Smoke Release Rates for Materials and Products Using an Oxygen Consumption Calorimeter. (ASTM International, West Conshohocken, PA), ASTM E 1354-16a.
- [11] ASTM (2017) Standard Test Method for Room Fire Test of Wall and Ceiling Materials and Assemblies. (ASTM International, West Conshohocken, PA), ASTM E 2257-17.
- [12] Bryant RA , Bundy MF (2019) The NIST 20 MW Calorimetry Measurement System for Large-Fire Research. (National Institute of Standards and Technology, Gaithersburg, MD), NISTTN 2077. <https://doi.org/10.6028/NIST.TN.2077>
- [13] Bryant RA , Bundy MF (2021) Improving the State-of-the-Art in Flow Measurements for Large-Scale Oxygen Consumption Calorimetry. *Fire Technol* 57(3):22. <https://doi.org/10.1007/s10694-020-01066-x>
- [14] Bryant RA (2018) Uncertainty estimates of tracer gas dilution flow measurements in large-scale exhaust ducts. *Flow Meas Instrum* 61:1-8. <https://doi.org/10.1016/j.flowmeasinst.2018.03.004>
- [15] ASTM (1999) Standard Test Method for Volumetric and Mass Flow Rate Measurement in a Duct Using Tracer Gas Dilution. (ASTM International, West Conshohocken, PA), ASTM E 2029-99.
- [16] Taylor JC (1987) Flow Measurement by Self-Averaging Pitot-Tubes. *Measurement and Control* 20(10):145-147. <https://doi.org/10.1177/002029408702001003>

- [17] Kabacinski M , Pospolita J (2011) Experimental research into a new design of flow-averaging tube. *Flow Measurement and Instrumentation* 22(5):421-427. <https://doi.org/10.1016/j.flowmeasinst.2011.06.006>
- [18] Rosemount (2006) Rosemount 485 Annubar Flow Handbook. (Rosemount Incorporated, Chanhassen, MN), Reference Manual 00809-0100-1191, RevCB.
- [19] Wright J, Kayl J, Johnson A, Kline G (2009) Gas Flowmeter Calibrations with the Working Gas Flow Standard. (National Institute of Standards and Technology, Gaithersburg, MD), NIST SP 250-80.
- [20] Ingle JDJ , Crouch SR (1988) *Spectrochemical analysis* (Old Tappan, NJ; Prentice Hall College Book Division), p Medium: X; Size: Pages: (608 p).
- [21] Christensen J (1990) The Brüel & Kjaer Photo-acoustic Transducer system and its Physical Properties: The Brüel & Kjaer Technical Review. 1.
- [22] NOAA (*Combined Sulfur Hexafluoride Data From the NOAA/ESRL Global Monitoring Division*) (National Oceanic and Atmospheric Administration, Boulder, CO). Available at <https://gml.noaa.gov/hats/combined/SF6.html>.
- [23] Lagus P, Butler P, Fleming K (2006) A Comparison of Tchebycheff, Equal Area and Tracer Gas Air Flow Rate Measurements. *29th NRC/DOE Nuclear Air Cleaning Conference*, (U.S. Nuclear Regulatory Commission, Washington DC, Cincinnati, Ohio).
- [24] Riffat S , Lee S (1990) Turbulent Flow in a Duct: Measurement by a Tracer Gas Technique. *Building Services Engineering Research and Technology* 11(1):21-26.
- [25] Riffat SB (1990) A Comparison of Tracer-Gas Techniques for Measuring Air-Flow in a Duct. *J Inst Energy* 63(454):18-21.
- [26] Silva AR , Afonso CF (2004) Tracer Gas Dispersion in Ducts - Study of a New Compact Device Using Arrays of Sonic Micro Jets. *Energy Build* 36(11):1131-1138. <https://doi.org/10.1016/j.enbuild.2004.04.005>
- [27] Zeng XY, Chi ZH, Zheng MG, Sun GG, Zhang GX, Wang JQ (2012) Experiment Research on Air Flow Rate Measurement Using Tracer Gas Method. *Sustainable Development of Urban Environment and Building Material, Pts 1-4*, Advanced Materials Research, eds Li H, Liu YF, Guo M, Zhang R, & Du J (Trans Tech Publications Ltd, Stafa-Zurich), Vol. 374-377, pp 520-523.
- [28] Adams DG, Lagus P, Fleming K (1996) Unit vent airflow measurements using a tracer gas technique. *24th DOE/NRC Nuclear Air Cleaning and Treatment Conference*, ed First M (U.S. Nuclear Regulatory Commission, Washington, DC, U.S. Nuclear Regulatory Commission, Washington, DC), pp 147-161.
- [29] Cheong KW (2001) Airflow Measurements for Balancing of Air Distribution System — Tracer-Gas Technique as an Alternative? *Building and Environment* 36(8):955-964. [https://doi.org/10.1016/S0360-1323\(00\)00046-9](https://doi.org/10.1016/S0360-1323(00)00046-9)
- [30] Lagus P, Flanagan B, Peterson M, Clowney S (1991) Tracer-Dilution Method Indicates Flowrate Through Compressor. *Oil and Gas Journal;(USA)* 89(8).
- [31] Grieve PW (1989) *Measuring ventilation using tracer-gases* (Brüel & Kjær).
- [32] ISO (1993) Fire Tests - Full-Scale Room Test For Surface Products. (International Organization for Standardization, Switzerland), ISO 9705:1993(E).
- [33] Cooper LY (1994) Some Factors Affecting the Design of a Calorimeter Hood and Exhaust. *Journal of Fire Protection Engineering* 6(3):99-112.

- [34] ISO (2008) Evaluation of Measurement Data - Guide to the Expression of Uncertainty in Measurement. (International Organization for Standardization, Switzerland), JCGM 100:2008.

Appendix A: Nomenclature

C_f	calibration constant for exhaust flow measurement
D	inner diameter of exhaust duct
$\Delta_c H$	net heat of combustion; lower heating value (LHV)
k	coverage factor
K_a	flow coefficient for averaging pitot probe
\dot{m}	mass flow
M	molecular weight
P	absolute pressure
ΔP	differential pressure
\dot{Q}	heat release rate
R	universal gas constant
s	non dimensional sensitivity coefficient
T	temperature
u	standard uncertainty
U	expanded uncertainty (95 % confidence interval, $k = 2.0$)
V	gas velocity
\dot{V}	volume flow
x	input quantity for measurement model
X	gas species volume fraction
y	output quantity of measurement model
Greek	
α	combustion products expansion factor
β	ratio of moles of combustion products to moles of oxygen consumed
ρ	gas density
ϕ	oxygen depletion factor, $\phi = f(X_{O_2}, X_{O_2}^o, X_{CO_2}, X_{CO_2}^o, X_{CO})$
σ	standard deviation (repeatability)
Subscripts	
c	combustion or combined
e	exhaust
eff	effective
i	index of gas species, averaging pitot probe, or input quantity
OC	oxygen consumption
Superscripts	
o	ambient conditions

Appendix B: Detailed Uncertainty Budgets

Estimates of measurement uncertainty were evaluated using the approximate methods described in the ISO GUM. [34] Measurement processes that were based on input measurements, x_i , were modeled as an output quantity, y :

$$y = y(x_1, x_2, x_3, \dots, x_N) \quad (\text{B1})$$

In the case that all input quantities, x_i , are uncorrelated, the relative combined standard uncertainty is given by

$$\frac{u_c(y)}{y} = \sqrt{\sum_{i=1}^N \left(s_i \frac{u(x_i)}{x_i} \right)^2} \quad (\text{B2})$$

Where $u(x_i)$ is the standard uncertainty for each input, and s_i is the associated dimensionless sensitivity coefficient given by

$$s_i = \frac{\partial y}{\partial x_i} \frac{x_i}{y} \quad (\text{B3})$$

Equation (B2) provides the propagation of uncertainty from each instrument and input parameter into the measurement model, Eq. (B1). The relative expanded uncertainty is defined as:

$$\frac{U(y)}{y} = k \frac{u_c(y)}{y} \quad (\text{B4})$$

Where $k = 2.0$, is the coverage factor for the 95 % confidence interval.

Table B.1 Example of an uncertainty budget for the volume flow determined using TGD at the 3 MW calorimeter.

Measurement Component, x_i	Value	$u(x_i)/x_i$	s_i	% Contribution
Injected Tracer Volume Fraction, $X_{T,I}$ (L/L)	1.0000	0.0001	1.0	0.0
Downstream Tracer Volume Fraction, $X_{T,D}$ (nL/L)	276	0.0112	-1.0	67.7
Upstream Tracer Volume Fraction, $X_{T,U}$ (nL/L)	0	-	0.0	0.0
Injected Tracer Volume Flow, $\dot{V}_{T,I}$ (m ³ /min)	3.185×10^{-4}	0.0007	1.0	0.3
Downstream Water Volume Fraction, $X_{H_2O,D}$ (L/L)	0.00884	0.0100	0.0089	0.0
Upstream Water Volume Fraction, $X_{H_2O,U}$ (L/L)	0.00894	0.0100	0.0	0.0
Repeatability (SDOM)	-	0.0060	1.0	19.5
Error Due to Inadequate Mixing	-	0.0048	1.0	12.5
$\dot{V}_{e,TGD}$ (m³/min)	1164	0.0136	Standard, $u_c(y)/y$	
		0.027	Expanded, $U(y)/y$	

Table B.2 Example of an uncertainty budget for effective exhaust velocity measured at the averaging pitot probes.

Measurement / Parameter, x_i	Value	$u(x_i)/x_i$	s_i	% Contribution
C_f (-)	1.028	0.014	1.0	90.9
K_a (-)	0.6271	0.0038	1.0	6.4
R (J/kmol K)	8314.47	0.0000	0.5	0.0
M_{air} (kg /kmol)	28.97	0.0035	-0.5	1.4
P_{amb} (Pa)	100 762	0.000 51	-0.5	0.0
ΔP_A (Pa)	27.16	0.0030	0.25	0.3
ΔP_B (Pa)	25.44	0.0030	0.25	0.2
$T_{e,A1}$ (K)	397	0.0051	0.13	0.2
$T_{e,A2}$ (K)	397	0.0051	0.13	0.2
$T_{e,B1}$ (K)	395	0.0051	0.12	0.2
$T_{e,B2}$ (K)	395	0.0051	0.12	0.2
$V_{e,\text{eff}}$ (m/s)	4.97	0.015	Standard, $u_c(y)/y$	
		0.030	Expanded, $U(y)/y$	

Table B.3 Example of an uncertainty budget for exhaust mass flow measured at the averaging pitot probes.

Measurement / Parameter, x_i (Units)	Value	$u(x_i)/x_i$	s_i	% Contribution
C_f (-)	1.028	0.014	1.0	88.3
K_a (-)	0.6271	0.0038	1.0	6.2
D_{eff} (m)	1.975	0.0013	2.0	2.8
R (J/kmol K)	8314.47	0.0000	-0.5	0.0
M_{air} (kg /kmol)	28.97	0.0035	0.5	1.3
P_{amb} (Pa)	100 762	0.000 51	0.5	0.0
ΔP_A (Pa)	27.16	0.0030	0.25	0.3
ΔP_B (Pa)	25.44	0.0030	0.25	0.2
$T_{e,A1}$ (K)	397	0.0051	-0.13	0.2
$T_{e,A2}$ (K)	397	0.0051	-0.13	0.2
$T_{e,B1}$ (K)	395	0.0051	-0.12	0.2
$T_{e,B2}$ (K)	395	0.0051	-0.12	0.2
$\dot{m}_{e,\text{eff}}$ (kg/s)	13.49	0.015	Standard, $u_c(y)/y$	
		0.030	Expanded, $U(y)/y$	